Aalto University
School of Electrical Engineering
Department of Communications and Networking

Huang Yi

Outdoor Signal Strength Measurement at TV Band and ISM Band in Otaniemi Campus

Master's Thesis
Espoo, August, 2013

Supervisor:
Professor Riku Jätti, Aalto University

Instructor:
Principle Researcher Jari Junell, NRC

Aalto University
School of Electrical
Engineering

Aalto University
School of Electrical Engineering
Department of Communications and Networking

ABSTRACT OF
MASTER'S THESIS

Author:	Huang Yi		
Title:	Outdoor Signal Strength Measurement at TV Band and ISM Band in Otaniemi Campus		
Date:	August, 2013	**Pages:**	x + 79
Professorship:	Radio Communications	**Code:**	S-72
Supervisor:	Professor Riku Jätti		
Instructor:	Principle Researcher Jari Junell		

TV white space technology is being intensively researched as it offers a solution that allows secondary usage of the local unused TV channels on a non-interfering basis to achieve a high spectrum efficiency.

This thesis studies the difference between TV band and ISM band outdoor propagation characteristics in Otaniemi campus area. The study aims to verify if the TV band signal could extend the service range with less transmitting power and if it has better propagation and building penetration characteristics than ISM band signal.

As part of our research we first perform a state-of-the-art review on TV white space technology including its features, promising applications and the evolution of regulation and standardisation. Then the measurement campaign set up is demonstrated based on the architecture of transmitter and receiver, the signal source and the antenna. Measurements were carried out by two transmitter locations and 49 receiver locations over distances up to 2.6 kilometers. The 'tcpdump' tool in OpenWrt system that embedded in Dlink box was used to measure the received signal characteristics for both bands.

The measurement results have been compared with the existing empirical propagation models and the differences between the model predicted and field measured data have been analysed. The results could be considered as a good basis for further theoretical research as well as for practical application research.

Keywords:	Propagation Measurement, TV Band, ISM Band, Outdoor, TV white space, Path Loss, OpenWrt, Empirical models, Dlink
Language:	English

Acknowledgements

This Master's Thesis is part of the Cognitive Radio Trial Networks (CoRTex) project in Nokia and has been written as a partial fulfillment for the Master of Science (Technology) degree at Aalto University, Finland.

As I come to an end of my master's thesis, I would like to reflect back and acknowledge everyone who made it possible. Most of all I want to thank my instructor principle researcher Jari Junell from Nokia for his instructions, guidance and invaluable advices and comments throughout my research work. This thesis would not have happened without his generous support. Then I would like to thank my supervisor, professor Riku Jäntti for the intriguing and in-depth comments throughout this thesis. Next I would also like to express gratitude toward my managers Niko Kiukkonen and Jussi Ruutu for giving me the chance to work in this project.

In addition, I must acknowledge my colleagues from Radio Prototyping and Piloting team: Markku Oksanen, Pasi Rinne-Rahkola and Miika Laaksonen who provided me technical and non-technical supports during my stay in Nokia Research Center. I also would like to show the gratitude to my friends Shen Yue, Gao Shan and all other Aalto Chinese for their helpful suggestions and constant encouragement. Thank you so much for listening and cheering me up anytime I have problems or worries.

My final thanks are reserved for my family especially my father Huang Bingxin, my mother Zhu Meifen and my boyfriend Wang Zhebin who have kept me motivated and given me all the love and support. Most importantly, I would like to dedicate this thesis to the memory of my beloved grandfather, Huang Arong, who I lost forever on April 7th, 2013.

Espoo August, 2013

Huang Yi

List of Figures

List of Tables

Contents

Chapter 1

Introduction

This chapter provides an introduction to our research work. Here first the motivation for our measurement campaign is given following which the spectrum status, possible solutions like cognitive radio technologies and TV white space technology are described. After that my own contributions to this thesis and the measurement campaign are presented, and finally structure of the thesis is outlined.

1.1 Motivation

The future will bring the need to deploy the available radio spectrum in more efficient manner. This trend has its roots in the increasing number of various radio systems, especially in the rapidly expanding number of consumers that have started to use wireless connectivity with their smartphones, laptops, notepads etc. Recent studies conducted by Cisco [3] showed that global mobile data traffic grew 2.3-fold in 2011, the growth rate is even higher than anticipated, and over 82% of the total mobile data traffic generated by smartphones which only represent 12% of global handsets. As the smart phones are widely adopted, the mobile data traffic is expected to have over 18-fold increase by the year 2016.

Traditional static spectrum allocation scheme only assigns bands to license holds, if the licensed services do not use their assigned bands, the spectrum resources will remain unutilized [4]. According to [5], the utilization of assigned spectrum ranges from 15% to 85% with a high variance in time at particular geographical locations. And the survey done by Islam [6] in 2008 shows that the average occupancy for the whole range of spectrum was found to be only 4.54% in Singapore. The radio spectrum is a finite natural resource. From technical point of view, it is possible to extend the

used radio spectrum to higher frequencies, but this requires typically more expensive hardware and introduces different kind of radio wave propagation features. Thus, it is inevitable to find a new spectrum allocation scheme to meet the growing demands.

One approach is to use cognitive radio technologies. Cognitive radio technology allows various radio network technologies to co-exist and to use the available local spectrum in a more flexible and efficient way than it is used currently. According to [7] [4] [5], despite the fixed quantity of spectrum resource, the available supply could be significantly expanded by allowing secondary usage. TV white space is the first emerging real application of cognitive radio technologies which allows licensed-exempt secondary users to access locally unused TV channels. It is an excellent example of more efficient usage of radio resources and co-existence of different systems.

According to [8], TV band signal could extend the service range with less transmitting power and has superior propagation and building penetration characteristics, especially in rural areas.

The object of the thesis is to validate the advantages of TV band signals presented in [8] and try to find a suitable propagation model to predict the propagation characteristics, which could be used in the TV white space testbed in Otaniemi in the future.

1.2 Own contribution

This thesis is part of the Cognitive Radio Trial Networks (CoRTex) project. The project is developing both the hardware and required software support for TV White Space (TVWS) radio network to be deployed to Otaniemi University Campus. My main contribution to this project is to conduct the outdoor propagation measurement in TV and ISM bands, which including systematically defining the measurement steps, software configuration and finding the critical hardware components based on the measurement requirements. The software configuration was mainly to get OpenWrt program run in our measurement environment. The hardware of transmitter and receiver were designed by Jari Junell, who is my instructor from Nokia side.

1.3 Scope of the thesis

The rest of the thesis is structured as follows. In chapter 2 the background information of TV white space including its features, evolution, regulation and standards developments are given and discussed. Radio propagation

characteristics and empirical propagation models are briefly introduced in Chapter 3. In chapter 4, the details of the measurement campaign including the architecture of transmitter and receiver, the antenna, the signal source, the measurement scenarios and the measurement implementing procedures are presented. The captured data processing, the measurement result and analysis are shown in chapter 5 and the conclusions and suggestions for the future work are given in chapter 6.

Chapter 2

TV white space

This chapter provides the background knowledge of TV white space for our measurement campaign. Here an introduction of the basic concept of TV white space and its features are given. Then the promising TV white space applications are discussed. After that the evolution of TV white space, including the regulation improvement, several trails around the world and industrial achievements are reviewed. Finally the related regulation and standardisation work are presented.

2.1 Concept

TV broadcast services operate on the licensed Very High Frequency (VHF) and Ultra High Frequency (UHF) radio spectrum which have a favourable propagation and penetration characteristics and can cover a wide area with relatively small transmission power. Even the spectrum is densely populated, there is still significant vacant spectrum in guard space or guard bands reserved for protecting the TV broadcast service area from interference generated by co-channel and adjacent channel TV stations at a given geographic area [9]. These vacant portions of the spectrum, known as TV white space, became available as both the United States Federal Communications Commission (FCC) and the Office of Communications (Ofcom) in UK proposed to exploit them by license exempt users devices to improved spectrum efficiency as long as they do not interfere any incumbent services, including TV broadcast and wireless microphone transmission. It is considered an ideal candidate solution for the spectrum shortage problem and estimated that up to 50% of the total broadcast band will be available for secondary uses in practice [10].

Currently most developed countries decide to switch-off the analogue ter-

restrial television network. This digital switchover is already completed in Finland and is underway in many other countries like UK [11]. After digital switchover, a portion of TV analogue channels freed up and these vacant channels cannot be considered as TV white space and will then be reallocated by regulators to other services. In Finland, the frequency band 790-862 MHz is planned for mobile broadband networks and band 470-790 MHz will be used for one additional nationwide multiplexer [12].

2.2 Features

The spectrum offers attractive propagation characteristics like high building penetration, wide coverage. According to the Friis transmission equation [13], for the same transmission power, TV white space can reach more than 4 times distance than 2.4 GHz band. Moreover, TV broadcast systems usually use high antennas, and the intended receivers need greater than 10 dB signal-to-noise ratio (SNR) to function [14]. These large SNR ratios simplify the technology needed to detect whether a channel is currently in use.

Despite these advantages, TV white space has some unique limitations. First, the propagation characteristics severely exacerbate the interference problem to the network. For example if two networks are very close to one another and operating on adjacent channels, the interference may cause network degradation. And if individuals and network service providers deployed networks in the same area and with no coordination, the interference problem will be harmful in this situation. Interfering transmitter has to detect TV transmission at very low levels not to cause problems to TV receiver by its own transmissions.

Second, there is spatial variation in spectrum availability. Available channels of TV white space depends on the location and the number of TV transmitters, and are affected by obstructions and constructions as well. That means one channel available at one point may not be available at another. A measurement in [15] showed that median number of channels available at one building but unavailable at another nearby building is close to 7. However, TV transmitters will not change their locations and spectrum frequently. Thus, the spectrum usage behaviour, transmit power and frequency in TV broadcasting service are relatively static in a particular region.

Third, the vacant channels will be non-contiguous and the channel width will also be different. The bandwidth of vacant spectrum depends on the density of TV stations and populations. Rural areas are likely to have larger bandwidth than urban areas [15]. The TV white space network must be designed to handle this spectrum fragmentation problem.

Moreover, the channel availability is subject to temporal variations because incumbent service can become active at any time without warning. So the TV white space network must be able to detect the signal and rapidly switch to a new available channel.

2.3 Promising applications

There are many discussions about what applications can be used in the TV white Spaces. In fact, most generally used applications for wireless communications could potentially be used in TV white space. Here we list several attractive applications considering commercial and technical aspects.

2.3.1 Rural connectivity

Up to now, in rural areas, especially mountainous and thickly forested country side has posed the greatest challenge to use broadband services [16]. TV white space frequencies could travel from miles away and provide affordable obstacle penetrating ability, which means Internet service providers will not need to build new infrastructure in order to deploy broadband in rural communities.

2.3.2 Internet of things

Industry forecasts estimate there will be more than 50 billion connected devices by 2020 [17], with a good proportion of these communicating and sharing information wirelessly, enabling a wide range of applications. Mobile broadband is too expensive for 'things' and mobile broadband also means battery powered devices would need to be charged far too often and all those sensors would load the cellular networks to such a level that there would be little network capacity left. Due to that, TV White space will unlock the potential of the Internet of things since it could cover large communication areas and will offer additional capacity which is not as good as higher frequencies but is adequate for 'things'.

2.3.3 Emergency and public safety network

This network can be used in emergency response and public safety organizations, such as police force, fire and medical teams responding to accidents,crimes, natural disasters and other similar events. Typical physical

topology for emergency and public safety networks is basically a mesh architecture that every existing public safety entity have a common radio communication system to command/control. All the end nodes (like fire fighters and paramedics) and cooperate with each other to efficiently execute missions. TV white space will make it possible due to the vast amount of bandwidth, secure and seamless communications. It will be accessible any time and anywhere with a cost-effective network. For example, a team of fire fighters searching for survivors in the building on fire, navigation and on-site operation assistance where digital maps can be downloaded from the main server to effectively plan and rescue the survivors. Once survivors are rescued, the cooperation radio system will control the video cameras to transmit images of the victim along with heart rate and other vital signs to paramedics to start immediate medical care.[18]

2.4 Evolution

Due to the attractive potential of TV white space, regulation committees and companies all over the world are highly involved in the TV white space research and development activities and there is considerable momentum currently. This section we take look at these important steps.

2.4.1 Regulatory

2.4.1.1 FCC

The idea of cognitive was first generated in 2002 when the Defence Advanced Research Projects Agency (DARPA) embarked on the Next Generation Communications Program (XG) to equip troops with radios, which could dynamically access vacant spectrum using cognitive radio techniques.[19]

Then Federal Communications Commission (FCC) in United States took action to draft the TVWS rules in May 2004 and in 2008, FCC adopted a report that established rules to allow license-exempt devices to operate in vacant television spectrum on a non-interfering basis [20]. It is an unprecedented move to open up new spectrum access rules.

2.4.1.2 Ofcom

The UK regulator Ofcom released a similar proposal as FCC to allow license exempt use of interleaved spectrum for cognitive devices in 2007 and proposed a number of technical parameters in a consultation published in 2009 [21]. At the same time in Finland, frequency range of 470-790 MHz

was allowed to test the cognitive radio system by Ministry of Transport and Communications [22].

2.4.1.3 Others

In European, the Radio Spectrum Policy Group (RSPG) of European Commission published a report and subsequent opinion on cognitive radio in 2011 that including sections on TVWS [23]. And the project team SE43 of European Conference of Postal and Telecommunications Administrations (CEPT) also dealt with TV white space in the UHF band and its main outcome so far is a report (ECC Report 159) focusing on calculations about the protection of incumbent service and technical requirements on the use of TV white space in January 2011 [24].

2.4.2 Trials

In UK, Ofcom have issued a test/experimental licence around Cambridge. This allows companies in the UK to demonstrate white space technology and its applications. On June 29, 2011, one of the largest commercial tests of white space network were conducted in Cambridge by a consortium comprising leading international and U.K. technology and media companies. In the demonstration, the Adaptrum whitespace system provided the broadband IP connectivity allowing a client-side Microsoft Xbox to stream live HD videos from the Internet and also a live Xbox/Kinect video chat was established between two Xbox/Kinect units connected through the same TV white space connection. These applications were demonstrated under a highly challenging radio propagation environment with more than 120 dB link loss through buildings, foliage, walls, furniture, people and with severe multipath effects. [25]

In another trial designed to show the feasibility and benefits of utilizing the spectrum located between TV channels for wireless data connections was conducted in Wilmington, North Carolina in January 2012. The network combines a Spectrum Bridge database with white space radios from KTS wireless, access points and cameras from various vendors that deployed in surveillance cameras, Internet access service, remotely monitor and live-streamed broadcasts. The applications can be expanded in Internet connectivity for local schools, medical monitoring, and other environmental monitoring in the future.

The latest trial was also conducted by the Cambridge TV White Spaces Consortium in April 2012 which explored and measured a range of applications-rural wireless broadband, urban pop-up coverage and the emerging 'machine-

to-machine' communication. It found that TV white spaces can be successfully utilized to help satisfy the rapidly accelerating demand for wireless connectivity.

In Singapore, the Information Communications Development Authority (IDA) designed several TV white space trials, named Cognitive Radio Venues (CRAVE), which will assist IDA in developing the regulatory framework for the use of TV band devices (TVBDs) [26]. From the trials, participants will be able to obtain real-world measurements, which would facilitate in the development of white space devices.

2.4.3 Industrial Achievements

Industry led research and development on TV White Space technology has been so far mainly focused in the USA, and is largely driven by the desire of important new players, including Google and Microsoft. The project from Microsoft called 'Networking Over White Space (KNOWS)' is a pioneer in TV white space research. The project enhanced the basic 'detect and avoid' sensing technology by using database approach. It also developed an API(Application programming interface) called WhiteSpaceFinder which is a web-based front end to visualize the availability of white spaces in particular area. The platform is powered by propagation modelling and an analysis engine which uses data exported by the FCC's publicly available CDBS database to determine the availability of white spaces based on TV tower information [27]. Spectrum Bridge and Sennheiser also developed similar white space available channel finder applications.

While Canada has already established a new broadband service for secondary, lightly licensed services over TV channels in the 512-698 MHz spectrum early 2010. This innovative service is called Remote Rural Broadband Systems(RRBS) [28]. The operating range can be up to 30 km. However, the receivers required to use this technology are not yet produced in sufficient quantities to make them affordable for the average consumer. But it gives very useful incumbent service protection experience for other committees [29].

In European, Neul, a company focuses on the area of Internet of the Things, developed a fully-functional wireless network in white space, enabling the world's first-ever smart electricity meter reading over a white space network. This is the first step towards smart electricity grids that will allow electricity supply to be more efficiently matched to real-time demand.[17]

2.4.4 Standards

2.4.4.1 IEEE 802.11af

IEEE 802.11 WLAN working group launched a TV white space project in 2009 and formalized a new standard called IEEE 802.11af which popularly known as Super WiFi/WiFi 2.0/WhiteFi [30]. The main difference from the well-known IEEE 802.11a/b/g standards is that IEEE802.11af will be a based on cognitive radio for operation in the TV white space. In order for whitefi to be able to operate, it is necessary to ensure that the system does not create any undue interference with existing television transmissions. The 802.11af task group is drafting an amendment to the IEEE 802.11 standard, including MAC/PHY modifications and enhancements to meet legal requirements for channel access and coexistence in the TV white space. The completed IEEE 802.11af standard will likely utilize the OFDM PHY proposed by project P80211ac [1].

2.4.4.2 IEEE 802.15.4m

In 2011 the IEEE 802.15 working group formed a new task group to develop an amendment to the 802.15.4 wireless personal area network (WPAN) standard for TV white space operations [31]. The new 802.15.4m task group is just beginning its work and will address device command and control applications including the smart grid in the TV white space band. IEEE 802.15.4m based devices may be used to enable many of the use cases which involved machine-to-machine communication. Targeted data rates are in the 40 kb/s - 2 Mb/s range. Another design target is to achieve high power efficiency.

2.4.4.3 IEEE 802.22

The IEEE 802.22 standard uses a centralized topology in which a base station serves up to 512 customer premises equipments (CPEs). Radio downlink is based on time division multiplexing, whereas uplink is based on orthogonal frequency division multiple access to support simultaneous transmission from multiple CPE units. The 802.22 standard incorporates many cognitive functions, both to protect incumbents and also for coexistence among 802.22 networks. These cognitive functions include channel classification and channel set management, quiet period scheduling for spectrum sensing, fusion of information from sensing, and database. Base stations follow spectrum etiquette to coexist with other networks in the area.

2.4.4.4 IEEE 802.19.1

The IEEE 802.19 Wireless Coexistence Working Group develops standards for coexistence of unlicensed devices between wireless standards [1]. Task group 1 is working on standard 'TV White Space Coexistence Methods' to specify radio technology independent methods for coexistence among dissimilar or independently operated TV band networks and devices. IEEE 802.19.1 coexistence system consists of three logical entities, coexistence enabler (CE), coexistence manager (CM), and coexistence discovery and information server (CDIS), which is schematically depicted in Figure 2.1 below. Each piece of information has a source which is a logical entity and the logical entity is defined by its functional role and its interfaces with other IEEE 802.19.1 coexistence system entities, or external elements. The 802.19.1 coexistence system will provide services subscribing networks to assist or implement the different coexistence solution steps.

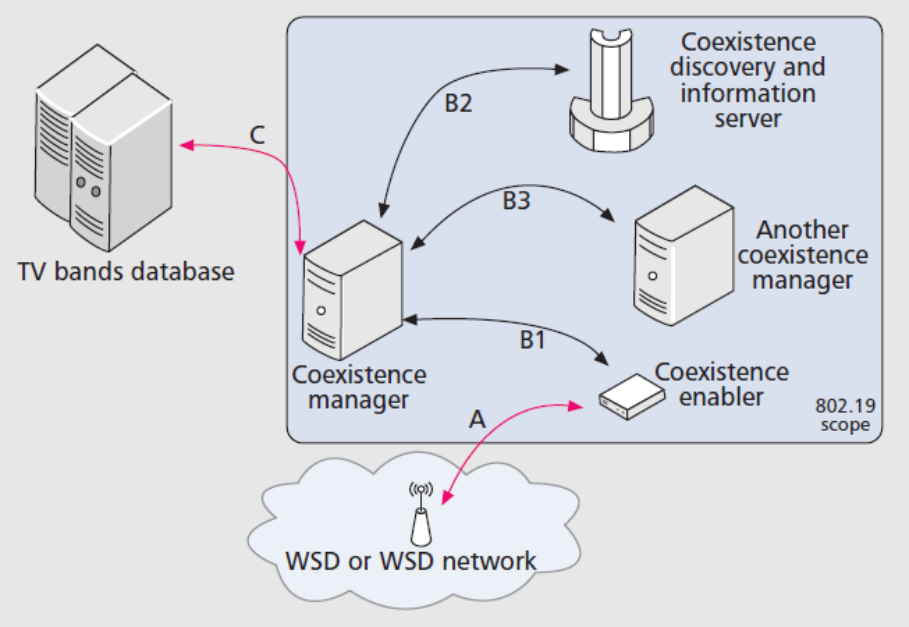

Figure 2.1: The IEEE 802.19.1 system architecture[1]

2.4.4.5 ETSI

Technical Committee on Reconfigurable Radio Systems of the European Telecommunications Standards Institute(ETSI) also develops standards for cognitive radio systems and reconfigurable radios(RRS). RRS are intelligent

radio devices which can scan unused spectrum that open up the opportunity to negotiate the second usage. Its purpose is to make more efficient and flexible use of spectrum to enhance user experience.[32]

Chapter 3

Radio propagation

Propagation characteristic is an important element when implementing the outdoor measurement. In this chapter, the basic propagation impairments caused by transmission channel, antenna and the transmission environment including the atmosphere and obstacles in the transmission path are presented. Then several outdoor empirical transmission models are discussed.

3.1 Propagation effects

When radio signal or electromagnetic wave propagate from one point on the Earth to another, or into various parts of the atmosphere, it will be affected by various phenomena, like reflection, refraction, diffraction, absorption, polarization and scattering. In this section we will briefly discuss those transmission impairments.

3.1.1 Attenuation

The strength of a signal falls off with distance over any transmission medium due to light scattering and atmospheric selective absorption of specific wavelengths. This reduction in strength or attenuation limits the transmission range of radio signals and is affected by the materials a signal must travel through.

3.1.2 Fading

Fading refers to the time variation of received signal power caused by changes in the transmission surrounding environment. Fading is the most challenging technical problem in designing a communication system. In a fixed environment, fading is affected by changes in atmospheric conditions. Whereas in a

mobile environment where either the receiving or transmitting antenna is in motion relative to the other, the relative location of various obstacles changes with time, causing complex transmission effects.

3.1.3 Interference

In any transmission event, a received signal will consist of expected signal and unwanted signals. These unwanted signals caused negative effects to the expected signals are referred to as noise or interference. The interference caused by various distortions imposed by the transmission medium and additional signal sources. Interference is a major limiting factor in any communications system performance.

3.1.4 Multipath

Multipath is the propagation phenomenon that due to radio signals reaching the receiving antenna by two or more paths. Depending on the differences in the path lengths of direct and reflected waves, the effects of multipath could be constructive and destructive. Destructive interference causes fading. The direct and reflected signals are often opposite in phase, which can result in a significant signal loss due to mutual cancellation in some circumstances. In digital radio communications, multipath can cause errors due to intersymbol interference(ISI). Equalisers are often used to correct the ISI.

Causes of multipath include atmospheric ducting, reflection and refraction, and reflection from water bodies and terrestrial objects such as mountains and buildings. We will briefly discuss several phenomena below.

3.1.4.1 Reflection

Reflection occurs when a electromagnetic wave hits on obstructions with properties(thickness, length) much larger than the wavelength of the radio wave. The reflection angle of the radio wave is the same as the incidence angle. The reflection loss depends on the electrical properties of the medium on both sides of the reflecting surface, the frequency used, the incidence angle and the polarization of the radio wave. The reflected waves may cause detrimental effect at the receiver.

3.1.4.2 Diffraction

Diffraction occurs when the radio wave strikes the edges or corners of obstacles. The secondary waves resulting from the obstructing surface radiates

into the space and even behind the obstacle, giving rise to a bending of waves around the obstacle, even when a line-of-sight path does not exist between transmitter and receiver. At high frequencies, diffraction, like reflection, depends on the geometry of the object as well as the amplitude, phase, and polarization of the incident wave at the point of diffraction.[33]

3.1.4.3 Scattering

Scattering occurs when the medium through which the wave travels consists of obstacle with dimensions that are small related to the wavelength, alters the radio wave propagation by retransmitting the signal in various directions. If there are a large amount of particles, a substantial amount of transmitter power can be lost. Scattering also causes polarisation cross coupling and therefore the received signal might not have the same polarisation as the transmitted signal. Reflection from an unsmooth surface causes scattering, as shown in Figure 3.1

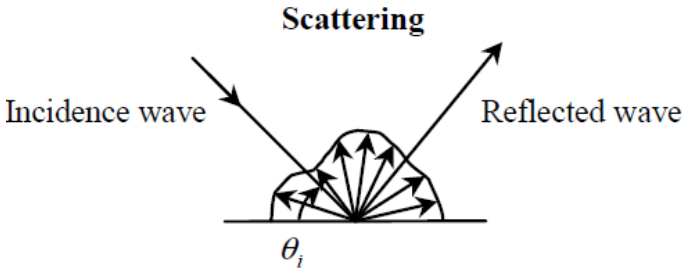

Figure 3.1: Scattering

3.1.4.4 Refraction

Refraction is defined as a change in direction of an electromagnetic wave resulting from changes in the velocity of propagation of the medium through which it passes. This may result in a situation in which only a fraction or no part of the line of sight wave reaches the receiving antenna.[33]

These four multipath propagation effects affect system performance in various ways depending on working environment and the way that a mobile unit moves through the medium. Diffraction and scattering are generally minor effects if there is a clear LOS between transmitter and receiver although reflection may have a significant impact. In cases where there is no LOS, diffraction and scattering are the primary means of signal reception.

3.1.5 Antenna effects

The antenna is a key component in propagation measurement which is used to convert between electric power and radio waves and usually be placed at the front-end of the transmitter and receiver. In transmitter, the antenna radiates the energy from the current as electromagnetic waves. In receiver, the antenna intercepts some of the power of an electromagnetic wave in order to produce a tiny voltage at its terminals, that is applied to a receiver to be amplified. The shape and radiation pattern of the antenna can determine the radio wave direction and how well input power can be converted to the radio wave in the specific direction which can be considered as 'gain' to antenna and 'transmit power' to the whole transmission system.

3.1.6 Atmospheric effects

Electromagnetic waves are absorbed in the atmosphere according to wavelength causing an additional loss. Two compounds are responsible for the majority of signal absorption: oxygen (O2) and water vapour (H2O). The actual amount of water vapour and oxygen in the atmosphere normally declines with an increase in altitude because of the decrease in pressure. A peak attenuation occurs in the vicinity of 22 GHz due to water vapor. At frequencies below 15 GHz, the attenuation is less. Climate changes like raining, also increase the signal attenuation. Total attenuation through the atmosphere at any frequency through unobstructed atmosphere is the sum of free space path loss, attenuation caused by oxygen absorption and attenuation caused by water vapour absorption.

3.2 Propagation models

In this section, empirical propagation models like Okumura-Hata model, ITU-R models and COST231 model that could be used in outdoor measurement campaign are discussed. Prediction of path loss is an important element of system design in any communication system. A reliable propagation model is one which calculates the path loss with small standard deviation. Suitable models will help network engineers and planners to optimise the cell coverage size and to use the correct transmitted powers. Empirical models use measurement data to model a path loss equation and use what are known as predictors.

3.2.1 Free space model

The free space propagation model is used to predict received signal strength when the transmitter and receiver have a clear, unobstructed line-of-sight path between them[13]. The path loss, which represents signal attenuation as a positive quantity measured in dB, is defined as the difference (in dB) between the effective transmitted power and the received power, and may or may not include the effect of antenna gains. The path loss for the free space model without antenna gains is given by:

$$L(dB) = 32.44 + 20log_{10}(freq) + 20log_{10}(dist) \tag{3.1}$$

where $freq$ is in MHz and $dist$ is in km.

3.2.2 One slope model

The commonly used one-slope log-distance model is

$$L(dB) = A + 10nlog_{10}(\frac{d}{d_0}) \tag{3.2}$$

where A denotes the path loss intercept, n is the path loss exponent which describes how fast the path loss increases with distance. The model parameters to be fitted are A and n.

The intercept is a fixed quantity is given by the free-space path loss formula[34]

$$A = 20log_{10}(\frac{4\pi d_0}{\lambda}) \tag{3.3}$$

where d_0 is the reference distance and λ is the wavelength in meters.

3.2.3 Okumura-Hata model

The Okumura model is based on measurements made in Tokyo city in 1960[35] at frequencies up to 1920 MHz and offers an empirical prediction method for path loss prediction. The original Hata model was published in 1980 by Masaharu Hata[36]. Hata took the information in the field strength curves produced by Okumura model and make it easier to apply by establishing a set of formulations.

For the suburban case, the path loss equation can be found as below:

$$L(dB) = 69.55 + 26.16log_{10}(f_c) - 13.82log_{10}(h_b) - a(h_m) + (44.9 - 6.55log_{10}h_b)\,log_{10}(d) - 2\left[log_{10}\left(\frac{f_c}{28}\right)\right]^2 - 5.4 \tag{3.4}$$

where

- $150 < f_c < 1500, f_c$ in MHz
- $30 < h_b < 200, h_b$ in meter
- $1 < d < 20, d$ in km

and $a(h_m)$ is the correction factor for mobile antenna height and it depends on the environment, here we assume the height of the mobile antenna is 1.5 m, and $a(h_m)$ is 0 dB. For frequency between 1500 and 2000 MHz, an Okumura-Hata extended model called COST231 model can be used[37]. The ITU-R P.529.3[38] also modified this Okumura-Hata model to fit the distance larger than 20 km, but is not widely adopted.

3.2.4 COST-Hata model

This model is derived from the Hata model and depends upon four parameters for the prediction of propagation loss: frequency, height of a received antenna, height of a base station and distance between the base station and the received antenna. The path loss is given by:

$$L(dB) = 46.3 + 33.9log_{10}(freq) - 13.82log_{10}(h_B) - a(h_R) + (44.9 - 6.55log_{10}(h_B))log_{10}(d) + C \quad (3.5)$$

$$a(h_R) = (1.1log_{10}(freq) - 0.7)h_R - (1.56log_{10}(freq) - 0.8) \quad (3.6)$$

where

- $1500 < freq < 2000, freq$ in MHz
- $30 < h_B < 200, h_B$ in meter
- $1 < d < 20, d$ in km
- $C = 0dB$ for medium sized city and suburban areas and $C = 3dB$ for metropolitan centres.

3.2.5 ITU-R models

ITU-R P Recommendation series describe radio propagation prediction methods in various aspects. Among them, recommendation ITU-R P.370[39] provides guidance on prediction of field strength for the broadcasting service for the frequency range 30 to 1000 MHz and for the distance range up to 1000

km, while ITU-R P.529[38] (based upon data for specific urban areas) on the prediction of point-to-area field strength for the land mobile service in the VHF and UHF bands centred around 150, 450 and 900 MHz and ITU-R P.1546[40] based principally on statistical analyses of experimental data in the frequency range 30 MHz to 3000 MHz and for the distance range 1 km to 1000 km. Recommendation ITU-R P.1146[41] is designed to achieve the level of accuracy needed for the preliminary planning of mobile radio and broadcasting services operating in the range 1 to 3 GHz. In Recommendation ITU-R P.1411[42], it defines four outdoor short-range propagation situations over the frequency range 300 MHz to 100 GHz.

The ITU-R P.1411 model described below is intended for propagation between low-height terminals where both terminal antenna heights are near street level well below roof-top height to calculate the basic transmission loss between two terminals. It includes both LoS and NLoS regions, and models the rapid decrease in signal level noted at the corner between the LoS and NLoS regions. The model includes the statistics of location variability in the LoS and NLoS regions, and provides a statistical model for the corner distance between the LoS and NLoS regions. It is reciprocal with respect to transmitter and receiver and is valid for frequencies in the range 300-3000 MHz.

The parameters required are the frequency f (MHz) and the distance between the terminals d (m).

Step 1: Calculate the median value of the line-of-sight loss:

$$L_{Los}^{median}(d) = 32.45 + 20log_{10}f + 20log_{10}(d/1000) \tag{3.7}$$

Step 2: For the required location percentage, p(%), calculate the LoS location correction:

$$\Delta L_{Los}(p) = 1.5624\sigma(\sqrt{-2ln(1-p/100)} - 1.1774), with\ \sigma = 7dB \tag{3.8}$$

Step 3: Add the LoS location correction to the median value of LoS loss:

$$L_{Los}(d,p) = L_{Los}^{median}(d) + \Delta L_{Los}(p) \tag{3.9}$$

Step 4: Calculate the median value of the NLoS loss:

$$L_{NLos}^{median}(d) = 9.5 + 45log_{10}f + 40log_{10}(d/1000) + L_{urban} \tag{3.10}$$

L_{urban} depends on the urban category and is 0 dB for suburban, 6.8 dB for urban and 2.3 dB for dense urban/high-rise.

Step 5: For the required location percentage, p(%), add the NLoS location correction:

$$\Delta L_{NLos}(p) = \sigma N^{-1}(p/100), with\ \sigma = 7dB \tag{3.11}$$

$N^{-1}()$ is the inverse normal cumulative distribution function. An approximation to this function, good for p between 1 and 99% is given by the location variability function $Q_i(x)$ of Recommendation ITU-R P.1546[40]. Alternatively, values of the NLoS location correction for p = 1, 10, 50, 90 and 99% are given in Recommendation ITU-R P.1411-6[42] section 4.3.

Step 6: Add the NLoS location correction to the median value of NLoS loss:

$$L_{NLos}(d,p) = L_{NLos}^{median}(d) + \Delta L_{NLos}(p) \tag{3.12}$$

Step 7: For the required location percentage, p(%), calculate the distance d LoS for which the LoS fraction F_{LoS} equals p:

$$d_{Los}(p) = \begin{cases} 212(log_{10}(p/100))^2 - 64log_{10}(p/100) & \text{if } p < 45 \\ 79.2 - 70(p/100) & \text{otherwise} \end{cases} \tag{3.13}$$

Step 8: The path loss at the distance d is then given as:

$$L(d,p) = \begin{cases} L_{Los}(d,p) & d < d_{Los} \\ L_{NLos}(d,p) & d > d_{Los} + w \\ L_{Los}(d_{Los},p) + (L_{NLos}(d_{Los}+w,p) - & \\ \qquad L_{Los}(d_{Los},p))(d - d_{Los})/w & \text{otherwise} \end{cases} \tag{3.14}$$

The width w is introduced to provide a transition region between the LoS and NLoS regions. This transition region is seen in the data and typically has a width of w = 20 m.

Chapter 4

The measurement campaign

4.1 Measurement objective

The aim of the measurement campaign was to compare the signal propagation performance of TV band and 2.4 GHz ISM band in areas with buildings and trees and to find the most suitable propagation model by fitting the measurement results to existing models. The measurement was conducted by transmitter beacon signals from a fixed transmitter to a mobile receiver in Otaniemi campus area where the TV white space testbed intended to install.

The frequency range of interest were 590 - 630 MHz and 2.4 GHz for TV band and ISM band, respectively. The TV test band license was issued by Ficora[1].

4.2 Transmitter

The architecture of the transmitter is shown in figure 4.1. In the transmitter end, a Dlink box was used as signal generator which would generate 2.4 GHz broadcast beacon signals. The Dlink box has two output ports and these two ports were connected to the TV band and ISM band transmitter chains.

The TV band transmitter chain contains attenuators, a mixer, a continuous wave generator, a power amplifier(PA) and a low pass filter(LPF). One of Dlink ports is connected to an attenuator in the TV band transmitter chain. The attenuator is used to limit the power that can damage the mixer where signal would be passed to next. The 2.4 GHz signal is downconverted to TV band signal with mixer and continuous wave generator. After that, the TV band signal is passed through another attenuator, then PA and LPF.

[1]Finnish Communications Regulatory Authority http://www.ficora.fi/

The ISM band transmitter chain contains an attenuator, a power amplifier(PA) and a band pass filter(BPF). The attenuator is connected to the other Dlink port and followed by power amplifier. Then the ISM band signals go through band pass filter.

Finally, the TV band signal and ISM band signal from TV band transmitter chain and ISM band transmitter chain, respectively, are processed separately before combining them at the diplexer and then passed to transmitting antenna.

The photo of our ready made transmitter is shown in figure 4.2a.

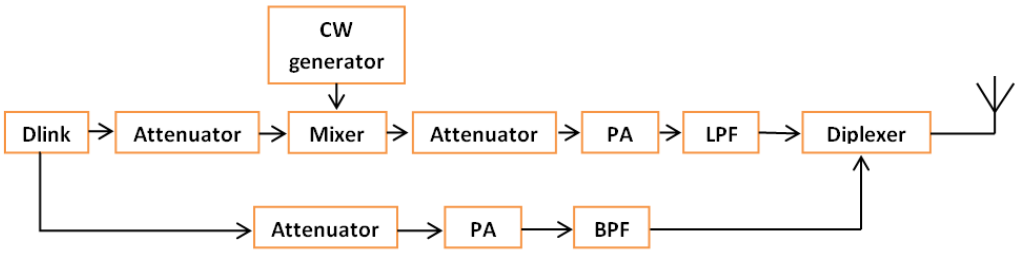

Figure 4.1: Transmitter architecture

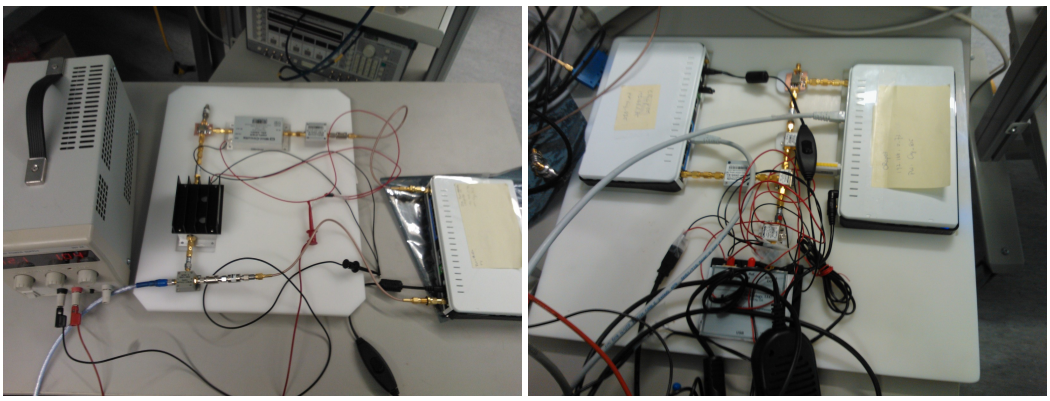

(a) Transmitter photo (b) Receiver photo

Figure 4.2: Photos of Transmitter and Receiver

Transmitter was placed in two locations. The first location was at the south balcony towards Innopoli on fourth floor of OIH building, as shown in figure 4.6a. The latitude was: 60°11'14.3"N and the longitude was: 24°48'56.7"E. The second transmitter location was at the opposite direction facing the bay, the antenna installation is shown in figure 4.6b. The latitude was: 60°11'15.9"N and the longitude was: 24°48'57.2"E.

4.3 Receiver

The receiver architecture used during measurements in transmission location 1 is shown in figure 4.3a and in transmission location 2 is shown in figure 4.3b.

In the receiver, the signal goes reversely as in the transmitter chain. The signal is received by antenna and passed to diplexer to split the TV band signal and ISM band signal. Then the signals are processed separately in the corresponding receiver chain.

In the first receiver, the TV band receiver chain contains low pass filter(LPF), low noise amplifier(LNA), mixer, band pass filter(BPF) and the Dlink box is used as receiver end. In the ISM band, the receiver chain only contains a Dlink box since there is no need to convert the receiving frequency and the Dlink box could sense the ISM band directly.

There are three advantages to use the Dlink box as receiver. First the size of the Dlink box is small so that it is easier to carry around than spectrum analysers in outdoor measurements. Second the power consumption is small. It is sufficient to get the supplied power from the car cigarette lighter. Then the network sniff tools could be installed in Dlink box directly using writable filesystem OpenWrt. The transmitting and receiving channel/frequency could be pre-defined in the configuration file. It has a significant effect on increasing the accuracy of received signals.

In the second receiver, the LNA is replaced to the position between antenna and diplexer to help better detecting ISM signals.

The photo of our ready made receiver is shown in figure 4.2b.

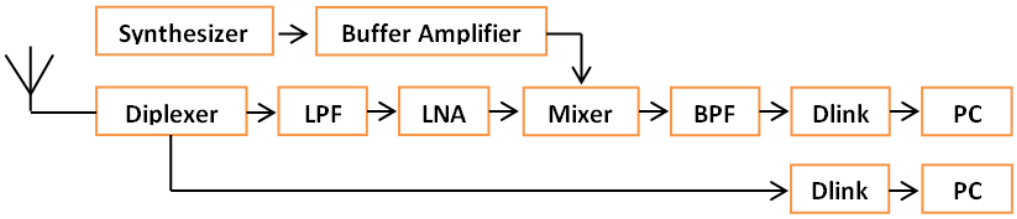

(a) Receiver architecture 1

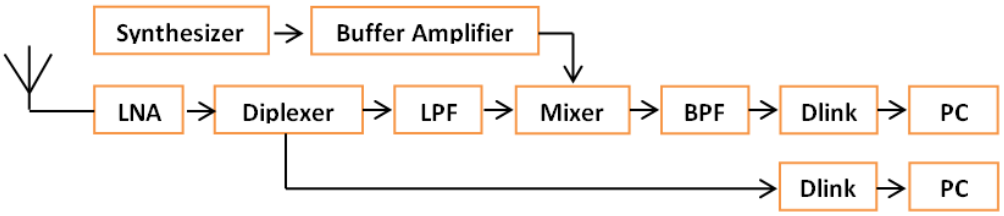

(b) Receiver architecture 2

Figure 4.3: Receiver architecture

4.4 Antenna

There are lots of antenna types with different shapes and radiation capabilities. Our aim was to measure the signal strength as a function of distance along different propagation paths. The effect caused by antennas itself should be mitigated. The dipole antenna has a radiation pattern, shaped like a toroid (doughnut) symmetrical about the axis of the dipole. The radiation is maximum at right angles to the dipole, dropping off to zero on the antenna's axis. This radiation pattern provides the most constant gain towards directions of interest. The exterior shape of the dipole antenna is shown in figure 4.4. At the receiver end, there is no need to adjust the antenna angle to get maximum signal strength when using the dipole antenna and same performance could be reached whether the receiver antenna face to the transmitter or back to it.

Figure 4.4: Antenna

The CD-300-3000 model omni-directional dipole antennas offered by Antenna Experts company were used. The operating frequency range of the antenna is 300 - 3000 MHz which covers both TV band and ISM band we

wanted. The horizontal beam-width is omni-directional while the vertical beam-width is 76 degree, as showed in Figure 4.5. The antenna gain is 1.5 dBi at 608 MHz and 0.5 dBi at 2462 MHz. The overall length of the antenna is 0.65 meter. The antenna operating environment is specified in the temperature range of -30 degrees to 70 degrees.

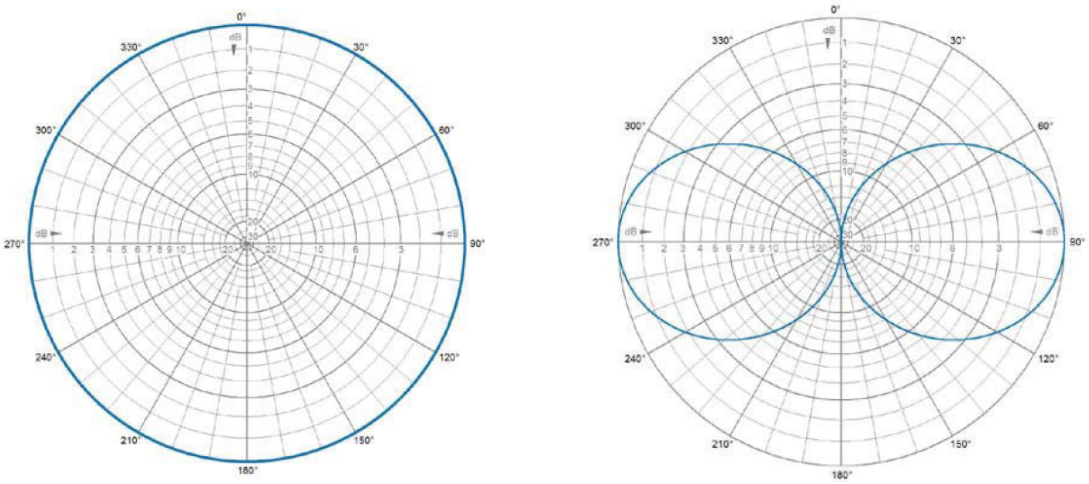

(a) Azimuth (b) Elevation

Figure 4.5: Dipole antenna radiation pattern

The antenna height to the ground at transmitter location 1 is 13.5 m and at transmitter location 2 is 13 m. At the receiver end, the antenna was installed on a car, as shown in figure 4.6c, and the height is 1.85 m.

(a) Tx location 1 (b) Tx location 2 (c) Rx antenna

Figure 4.6: Antenna installation photo

4.5 The signal source

The Dlink dir-825 model, as shown in figure 4.7 was implemented as both the signal generator at the transmitter end and measurement equipment at the receiver end. Both 2.4 GHZ and 5 GHz bands signals could be generated simultaneously while in our measurement only 2.4 GHz signal was used. The hardware features are listed in the table 4.1 where we could find that it runs on the atheros chip and has four LAN ports.

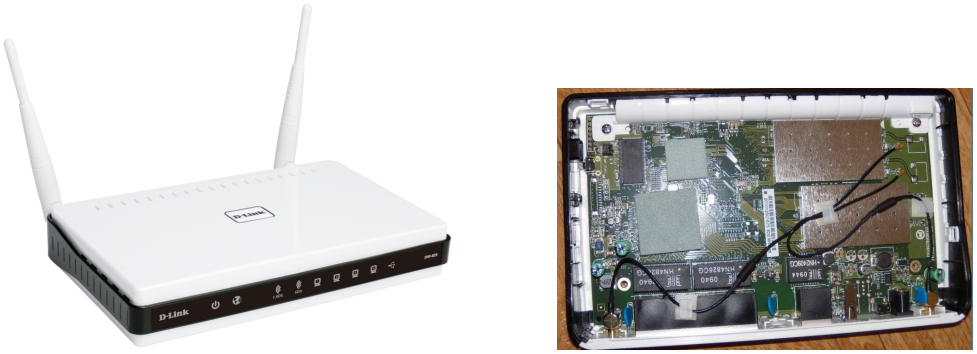

(a) exterior (b) interior

Figure 4.7: Dlink box

The dlink box was flashed using OpenWrt firmware and one of the boxes was configured as transmitter to generate 2.4 GHz broadcast beacons at 19 dBm transmission power and one as the receiver. At the receiver, 'tcpdump' wireless sniff software was used to capture the signals.

The OpenWrt introduction could be found in Appendix B. So as the network and wireless configuration details of the DLink box as transmitter and receiver, which could be found in Appendix B.3. The transmitter was named as 'CRap06' and the IP address was configured to 192.168.0.76. The other two Dlink box were used as receivers with same configuration but different IP address. Both transmitter and receivers were operated in channel 11(2.462 GHz). The transmitter was in 'ap' mode and receivers were in 'sta' mode.

4.6 Measurement scenarios

The measurements were performed along the road in Otaniemi and over Laajalahti gulf. Otaniemi is a campus of Aalto University with a compact $2km \times 2km$ area located in Espoo(Finland's second largest city) along the

Architecture	MIPS
Vendor	Qualcomm Atheros
Bootloader	U-boot
System-on-chip	AR7161 rev 2(MIPS 24Kc v7.4)
CPU/Speed	24Kc v7.4 680 MHz
Flash-Chip	Spansion S25FL064A
Flash size	8192 KB
RAM	64 MB
Wireless	2×Atheros AR922X 2.4/5 GHz 802.11abgn
Switch ports	5,numbers 0-3 are Ports 4 to 1 as labelled on the unit, 5 is the internal connection to the router itself
Ethernet	RealTek RTL8366S Gigabit w/port based vlan support
Internet	n/a
USB	yes 2×2.0(only 1 header to the outside)
Serial	yes
JTAG	yes

Table 4.1: Dlink dir-825 hardware[2]

west coast of Laajalahti gulf. It is in arid climates and the temperature is around 6 degrees outside in mid-April. The rainbow map according to the terrain elevation of our measurement area is shown in figure 4.8b. The elevation from the sea level varies from 5 m to 28 m in land area and 0 m in the gulf. The data is based on SRTM (Shuttle Radar Topography Mission)[2] and the accuracy could be referred to [43], which contains a detailed analysis and discussion.

Both land-only and land-lake propagation paths were covered in the measurement campaign. The lake path was measured to indicate LOS (Line Of Sight) path loss. The measured area was from the ground area near OIH building to over the bay and the distance varied from several meters to 2.6 km.

The measurement locations were selected from the place close to the transmitter to the place as far as where the signal could be detected in all the directions. The locations that measured were marked on the map in Appendix D.1.

Since the measurement was no laboratory measurement, but field mea-

[2]SRTM is an international project spearheaded by the National Geospatial-Intelligence Agency (NGA) and the National Aeronautics and Space Administration (NASA)

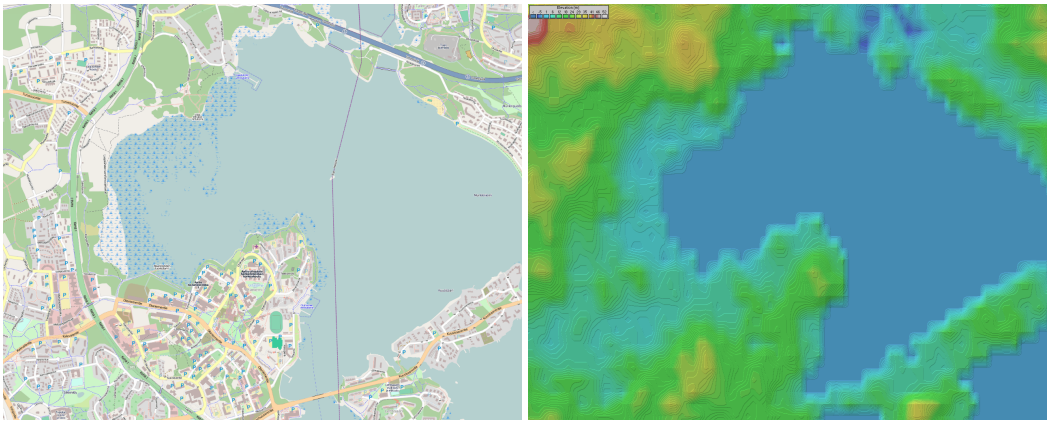

(a) Otaniemi openstreet map (b) Otaniemi elevation map

Figure 4.8: Measurement scenario map

surement in real life circumstances, interference from other signals, additional attenuation caused by multi-story buildings, leafless trees, high chimneys, vehicles etcetera should be expected and be taken into account. Measurements were conducted mainly on the road and parking areas.

The channel bandwidth of DVB-T signal is 8 MHz in Europe. Due to the restricted condition, we were not able to have those signals. The channel bandwidth in both bands of this measurement campaign were 22 MHz.

4.7 Data collection

PCs with Ubuntu operation system were used to connect to the Dlink receivers to control the data collection. To start the control, the command terminal should be connected to the Dlink receiver by login to OpenWrt using 'ssh' protocol. The data of all measured locations were collected in the wireless monitor mode. The command below was used to detect the signal.

```
tcpdump -tttt -i mon0 -c 10
        "(ether host MAC_address)&&(link[0]==0x80)"
```

'link[0]==0x80' is used to specify only beacon signals would be captured. '-c 10' is the number of packets we expect to capture.

The data collection script would be executed with a location number after confirming that the signal could be detected in that location. The script used to collect data was previously stored in the USB stick. The USB sticks were mounted to the Dlink receivers with one for each. All the measured data could be stored automatically to corresponding mounted USB stick.

The scripts could be found in Appendix C. The default number of packets we expected to capture in the measurements was 1000 in each file and 5 files in each location. However, the field measurement in real life circumstances would experience interference and in some locations, the wanted signal would be blocked, only few leaking packets could be detected. In this situation, we took as many samples as we could at those locations. During the measurement, the car only moved in a small range which was less than 5 m.

4.8 Coverage simulation

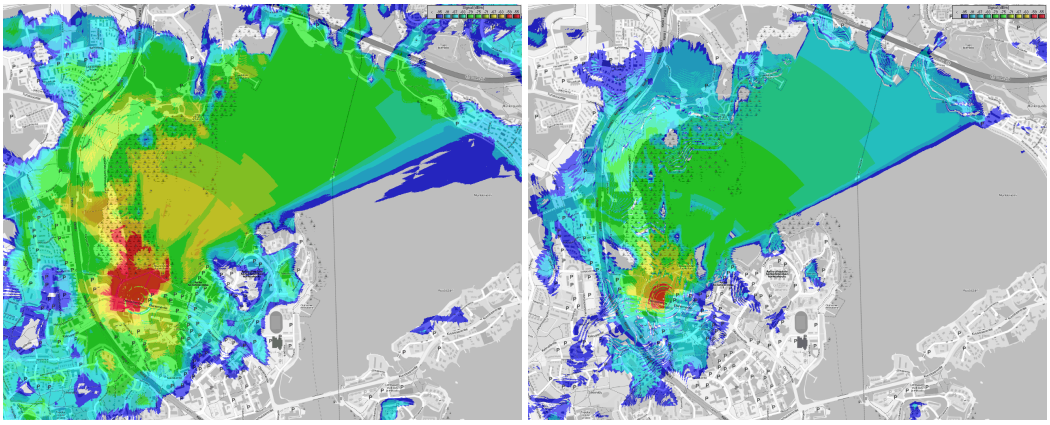

(a) TV band (b) ISM band

Figure 4.9: Coverage simulation maps

Before the measurement campaign, a radio propagation simulation was done by Radio Mobile propagation simulation software developed by Roger Coudé[3]. The simulation was based on the key parameters in table 4.2 while using 608 MHz in TV band and 20 MHz bandwidth for both bands. The contour plot of variation in received signal strength (dBm) from transmitter location 1 is shown in figure 4.9 and the signal varies from -95 dBm to -55 dBm. Free space propagation was selected in the software. As the result, in both the coverage maps, the north-west area was covered with better signals at both the TV band and ISM band than the south-east area while signals at TV band are stronger in all directions than ISM band signals. The coverages maps were used as a reference when conducting the field measurement campaign.

[3]http://radiomobile.pe1mew.nl/?Welcome...

Parameter	**TV band**	**ISM band**	**Note**
Frequency(MHz)	608 Tx1/ 618 Tx2	2462	
Transmit power(dBm)	20.52	23.07	Measured by spectrum analyzer after diplexer
Tx cable loss(dB)	0.58	1.14	Cable between diplexer and transmit antenna
Tx antenna gain(dBi)	1.5	0.5	Measured by spectrum analyzer
Tx1 antenna location	$60°11'14.3''N, 24°48'56.7''E$		Measured by Lumia 820
Tx2 antenna location	$60°11'15.9''N, 24°48'57.2''E$		Measured by Lumia 820
Tx1 antenna height(m)	13.5		Uncertainty:$\pm 0.5m$
Tx2 antenna height(m)	13		Uncertainty:$\pm 0.5m$
Bandwidth(MHz)	22	22	
Rx antenna height(m)	1.85		Uncertainty:$\pm 0.2m$
Rx antenna gain(dBi)	1.5	0.5	
Rx cable loss(dB)	0.74	1.16	Cable between receiver antenna and diplexer
Rx chain gain(dB)	12.5	-1.4 Rx1/ 13.2 Rx2	Measured by spectrum analyzer

Table 4.2: Key parameters

Chapter 5

The measurement results

In this chapter, the signal strength obtained from our measurement campaign are demonstrated and evaluated. First the data processing procedures to extracting signal strength in corresponding locations are provided. Then the measurement results after data processing are evaluated and discussed. Finally a laboratory calibration is implemented and the results is presented.

5.1 Data processing

The data files were stored in corresponding USB stick by default when executing the data collection script. These data files were later processed using shell script and analysed by Octave. The post-processing was done in following steps:

1. Conversion to a readable file format;
2. Extracting RSS(Received Signal Strength) value;
3. Filtering data;
4. Application of calibration factors;
5. Loading location data;
6. Statistical processing.

5.1.1 Conversion

The original data files were in '.dump' format. The contents of the file could be checked using wireshark[1] software. In the following statistical processing

[1]http://www.wireshark.org/

steps, like extracting the received signal strength values, filtering the data and application of calibration factors, required the reading of a large amount of data. To avoid unnecessary manual labour, batch processing of the data files is needed. The data files should be transferred to readable and easy-access file format. The command below was used which could transfer '.dump' file to plain text file (.txt).

```
sudo tcpdump -nettvvv -s 0 -r orignalfile.dump > file.txt
```

The plain text format after conversion is shown in the figure 5.1 below. The signal strength value is in the column 9 which would be extracted in the following steps. This step greatly simplified further statistical processing when a huge amount of data have to be read and processed.

```
1366182288.666627 550299051us tsft 1.0 Mb/s 2462 MHz 11b -49dB signal antenna 1 0us BSSID:00:18:e7:da:a4:2a
DA:ff:ff:ff:ff:ff:ff SA:00:18:e7:da:a4:2a Beacon (CRap06) [1.0* 2.0* 5.5* 11.0* 6.0 9.0 12.0 18.0 Mbit] ESS CH: 11
1366182288.769027 550401450us tsft 1.0 Mb/s 2462 MHz 11b -49dB signal antenna 1 0us BSSID:00:18:e7:da:a4:2a
DA:ff:ff:ff:ff:ff:ff SA:00:18:e7:da:a4:2a Beacon (CRap06) [1.0* 2.0* 5.5* 11.0* 6.0 9.0 12.0 18.0 Mbit] ESS CH: 11
1366182288.871425 550503852us tsft 1.0 Mb/s 2462 MHz 11b -48dB signal antenna 1 0us BSSID:00:18:e7:da:a4:2a
DA:ff:ff:ff:ff:ff:ff SA:00:18:e7:da:a4:2a Beacon (CRap06) [1.0* 2.0* 5.5* 11.0* 6.0 9.0 12.0 18.0 Mbit] ESS CH: 11
1366182288.973825 550606251us tsft 1.0 Mb/s 2462 MHz 11b -47dB signal antenna 1 0us BSSID:00:18:e7:da:a4:2a
```

Figure 5.1: Plain text format

5.1.2 Extracting RSS value

The received signal strength is the most interest parameter in the data files. The future statistical processing and data analysis mainly based on this parameter. To simply the data files, the second step in data post-processing was to extract the received signal strength value from multiple data in the plain text file. Command 'awk' was used here.

```
awk '{print $9}' file.txt > rssi-file.txt
```

The 'print' command was used to output text from 'file.txt' and saved the output text to destination file.

Batch processing was applied to both step 1 and step 2 with a shell script. The shell script could be found in Appendix C.

5.1.3 Filtering data

After all the captured signal strength values have been extracted, the following processing step was used to trim the data. The measurement data followed a normal distribution in each location. In order to get rid of the

Calibration factor	TV band	ISM band
Antenna gain	1.5 dBi	0.5 dBi
Cable loss	0.74 dB	1.16 dB
Receiver chain gain	12.5 dB	-1.4 dB for Rx1 13.2 dB for Rx2

Table 5.1: Calibration factors

extreme unstable signal values which caused by the slightly changing of the environment, eg. walking people, passing trucks, etc, filtering these data was a necessity. The way we did to trim those data files was first sorting all the values and then taking only the part between 20% and 80% for further processing.

5.1.4 Application of calibration factors

The received signal strength in data files was captured by Dlink receiver. Calibration should be applied before the statistical processing.

The application of the calibration factors could be introduced in a fairly easy way using Octave. The calibration factors that had to be applied were:

1. Antenna gain;
2. Cable loss;
3. Receiver chain gain.

The value of each calibration factor could be referred to table 5.1.

5.1.5 Loading location data

The following step was to load the location data which including latitude, longitude and elevation. The propagation characteristics can only be evaluated under the condition of a distance, otherwise the analysis of the received signal strength makes no sense. The latitude and longitude were measured by Nokia lumia 820 in degree minute second format. The elevation was calculated in RF propagation simulation software based on SRTM elevation data and latitude-longitude pairs. Loading the location data manually to a file in the format as below: The location file could be loaded to Octave script and be used to calculate the distance between transmitter and receiver. The ground

Loc	Lati degree	Lati minute	Lati second	Longi degree	Longi minute	Longi second	Elev(m)
1	60	11	12.6	24	49	2.6	9.6
2	60	11	11.9	24	49	15.6	12
... ...							

Table 5.2: Location data format

distance $dist_{ground}$ could be calculated by two sets of GPS coordinates. The propagation distance was calculated in the way as below:

$$distance = \sqrt{(dist_{ground})^2 + (Hant_{tx} + ele_{tx} - Hant_{rx} - ele_{tx})^2} \quad (5.1)$$

while $Hant_{tx}$ is the transmitter antenna height to the ground level, ele_{tx} is the elevation of the transmitter location from sea level to ground level, $Hant_{rx}$ is the receiver antenna height to the ground level, ele_{tx} is the elevation of the receiver location.

5.1.6 Statistical processing

The first purpose of the statistical processing step is to make a path loss vs distance distribution diagram of all measurements in the measurements. All the data files were loaded to Octave workspace to get the average, maximum, minimum value of the received signal strength at each location. After that the corresponding propagation loss could be calculated using those values with the transmission power. The measurement results were sorted according to their distance to the transmitter. Empirical propagation models would be present as a comparison to the measured data.

5.2 Results analysis

In this section, the general results we got from the measurement campaign are presented and discussed first. Then a comparison between the measured signal strength and the simulated one from coverage map are given. Following the measured propagation path loss will be compared to empirical propagation models. The aim is to find out which model could give the best agreement with the measured propagation data.

5.2.1 General results

In this part, the received signal strength values of each location are given first. Next the difference between the measured results and the coverage simulation results mentioned in Section 4.8 are discussed. Then the figure of measured propagation loss vs distance is presented and discussed.

5.2.1.1 Received signal strength

The received signal strength values got from the measurement campaign are listed in table 5.3 and 5.4. Among all the locations, location 5, 8, 15, 30, 31, 42, 46, 47 and 48 showed interesting signal situation. The details of these locations can be seen in table 5.5. Location 8 is at the end of the parking area and signal could not be detected anywhere else in that parking area except location 8. There is a small between the transmitter and location 8, the average height of the tree is about 15 meters. The trees act as obstacles in the radio path causing both absorption and scatter of radio signals. Location 15 is close to location 16 and in the opposite side of location 17 and location 18. In location 16, 17 and 18, the TV band signal was quite stable but in location 15, only several packets were captured in TV band. The signal might be block by the sharp corner of the building behind. Location 42 could be considered as a leaking point due to that only in a very special point, the signal could be detected and if the vehicle move a bit forward or backward, the signal lost. The leaking signal might caused by the reflection of the buildings. Location 47 was located over the bay and could be considered as a LOS point. However, in the real measurement, there is trees along the bay area and the trees might block the signal. Signals could be detected might due to the leakage through the trees and the location 47 is in a relatively higher elevation.

TV band experiences less free space loss and has a better penetrating ability, the location where ISM band signal could be detected should have a better TV band signal. However, in the field measurement,there were some strange situations showed in location 5, 30, 31 and 46, that ISM band signals were more stable and could be detected more easily than TV band signals. This led us to examine the spectrum near the TV band test signal. As a result, a TV interferer signal was detected at 586 MHz. The signal level was about -49 dBm at antenna connector in transmitter 1 and 2 or 3 dB less in transmitter 2. The interferer signal might came from Kivenlahti TV station which located 9.4 km west of our transmitter with ERP(Effective Radiated Power) of 35 kw (75.4 dBm). A calibration was implemented in laboratory which could confirm that the effect caused by the interference in

Loc	**ISM band**(dB)			**TV band**(dB)			**Note**
	Max	Mean	Min	Max	Mean	Min	
1	-62.9	-65.6	-68.9	-66.3	-68.2	-71.3	
2	-65.9	-72.9	-80.9	-80.3	-83.2	-84.3	
3	-74.9	-77.4	-79.9	-77.3	-79.6	-83.3	
4	-76.9	-78.1	-79.9	-85.3	-86.3	-87.3	Nlos
5	-84.9	-85.9	-86.9	x	x	x	Nlos
6	x	x	x	-81.3	-82.7	-84.3	Nlos
7	-82.9	-85.4	-87.9	-83.3	-84.6	-85.3	Nlos
8	x	x	x	-85.3	-86.8	-88.3	Nlos
9	-49.9	-52.7	-55.9	-60.3	-61.6	-63.3	
10	-74.9	-75.8	-76.9	-75.3	-75.5	-76.3	
11	-69.9	-71.7	-72.9	-77.3	-77.9	-78.3	Nlos
12	Test location						
13	Test location						
14	-72.9	-75.4	-76.9	-62.3	-66.3	-70.3	Nlos
15	x	x	x	-80.3	-80.8	-84.3	Nlos
16	x	x	x	-82.3	-84.5	-86.3	Nlos
17	x	x	x	-71.3	-74.2	-76.3	Nlos
18	x	x	x	-84.3	-86	-88.3	Nlos
19	x	x	x	-82.3	-83.1	-85.3	Nlos
20	x	x	x	-78.3	-81	-83.3	Nlos
21	x	x	x	-84.3	-84.8	-85.3	Nlos
22	x	x	x	-79.3	-80.7	-81.3	Nlos
23	x	x	x	-81.3	-82.5	-84.3	Nlos
24	-59.9	-61.2	-62.9	-62.3	-68.1	-72.3	
25	-61.9	-65.3	-70.9	-55.3	-56.6	-58.3	
26	-77.9	-80.1	-82.9	-69.3	-70.8	-72.3	Nlos
27	-87.9	-88.5	-89.9	-83.3	-84.8	-86.3	Nlos
28	-78.9	-80.7	-82.9	-71.3	-73	-76.3	Nlos

Table 5.3: Received signal strength Tx1

Loc	**ISM band**(dB)			**TV band**(dB)			**Note**
	Max	Mean	Min	Max	Mean	Min	
29	-41.5	-43.9	-46.5	-44.3	-45.1	-46.3	
30	-82.5	-83.2	-83.5	-89.3	-89.8	-90.3	Over the bay
31	-88.5	-90.2	-91.5	x	x	x	Over the bay
32	-86.5	-88.9	-90.5	-80.3	-81.7	-82.3	Nlos
33	x	x	x	-82.3	-83.7	-84.3	Nlos
34	-81.5	-82.6	-83.5	-73.3	-74.4	-75.3	Nlos
35	-92.5	-94.4	-95.5	-81.3	-82	-83.3	Nlos
36	-85.5	-92.9	-98.5	-66.3	-68.2	-69.3	
37	-96.5	-101	-105	-67.3	-68.7	-70.3	Nlos
38	-98.5	-102	-104	-82.3	-83.8	-85.3	Nlos
39	-85.5	-90.3	-98.5	-59.3	-60.6	-62.3	
40	-72.5	-73.8	-75.5	-62.3	-63.7	-64.3	
41	x	x	x	-84.3	-85.3	-86.3	Nlos
42	x	x	x	-83.3	-84.7	-86.3	Nlos
43	-93.5	-95.4	-97.5	-78.3	-79.3	-80.3	Nlos
44	-83.5	-86.5	-90.5	-72.3	-73.1	-74.3	
45	-53.5	-61.3	-68.5	-49.3	-50.9	-54.3	
46	-88.5	-89.9	-91.5	x	x	x	Over the bay
47	-92.5	-92.5	-93.5	-90.3	-90.9	-92.3	Over the bay
48	x	x	x	-84.3	-84.3	-85.3	Nlos Over the bay
49	-92.5	-93.4	-94.5	-87.3	-88.5	-89.3	Nlos Over the bay

Table 5.4: Received signal strength Tx2

Loc	**Direction to TX**	**Distance**	**Situation**
5	North-west	0.3356 km	no TV signal, capture ISM band signal slowly
8	South	0.2217 km	capture TV band signal slowly, no ISM band signal, signal only be detected at the end of the parking area
15	South-east	0.4762 km	capture TV band signal slowly, no ISM band signal
30	North-east	1.8532 km	capture ISM signal faster than TV signal, only few packets in TV band, a small movement will loss the signal
31	North-east	2.3975 km	capture only ISM signal
42	North-east	0.5065 km	only TV signal detected in a sharp point, a small movement will loss the signal
46	North-east	2.6233 km	only ISM signal detected, capture in normal speed, the farthest location measured
47	North-east	1.8509 km	capture TV signal in normal speed, only several ISM band packet captured, a small movement will loss the signal
48	North-west	0.9218 km	only few TV packets captured, no ISM band signal

Table 5.5: Interesting locations

TV band was significant. With this interferer signal, the TV test band signal at its sensitivity level was not able to be measured except in very rear cases, where the interferer signal would be blocked a lot. The calibration set-up and measurement details in the laboratory could be referred to Section 5.3.

5.2.1.2 Propagation loss

The general measured propagation loss versus the distance to the transmitter is shown in figure 5.2a. In each location, the measured data contains the mean, maximum and minimum value in that location. As can be seen both TV band and ISM band are following the same tendency: the propagation loss increases as the distance does. The ISM band generally experiences about 10 dB more propagation loss compared to TV band. The path loss vs distance in logarithm can be seen in figure 5.2b.

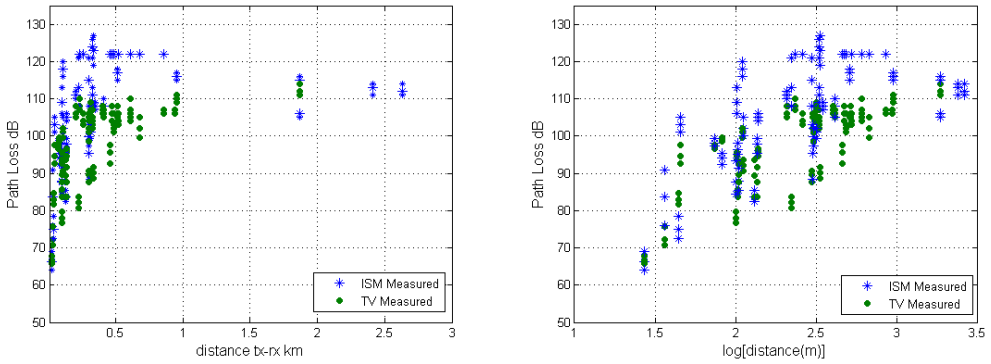

(a) Passloss vs distance (b) Passloss vs distance in log

Figure 5.2: Measured propagation loss

5.2.2 Comparison of measurements and simulations

When comparing to the coverage simulation results, in TV band, only the signal within the light green area(as shown in figure 4.9a) could be detected partly, while in ISM band, the signal could be detected within the light blue contour(around -83 dBm in figure 4.9b) and the smallest value could be detected is -105 dBm at location 37, which located at the edge of light and dark blue contour and is about 20 dB smaller than predicted. The signal various greatly around building corners and the prediction compared to measured values also shows the effect. The range of measured signal strength and simulated could be referred to table 5.6 and table 5.7. The

mean of measured signal strength and simulated values could be found in table 5.8 and table 5.9. The standard deviation of error between the mean values of measurements and simulations is 13.80 for ISM band and 12.46 for TV band.

5.2.3 Free space model

Figure 5.3a and figure 5.3b give the comparison results of measured path loss with free space propagation model. The dash and solid line represent the free space propagation loss at corresponding distance for ISM band and TV band. As can be seen, at distance beyond 1 km, the measured data is close to the free space loss curve in ISM band, but the receivers are still suffered from excess propagation loss than in free space. While in TV band, the measurement results exceed free space path loss by 8 to 33 dB. That may due to the blockage of dust and diffraction over the top of the trees twigs. As we known, free space is assumed as a vacuum environment, there are no elements in the propagation environment. The appearance of any physical substance on the propagation path could increase the propagation loss. More buildings and trees come into the way between the transmitter and receivers, the more excess propagation loss will be experienced. This explains the big discrepancy between the measured values and the free space curve shown in the figures. The standard deviation error between the free space model and mean measured path loss is 23.78 for ISM band and 24.73 for TV band.

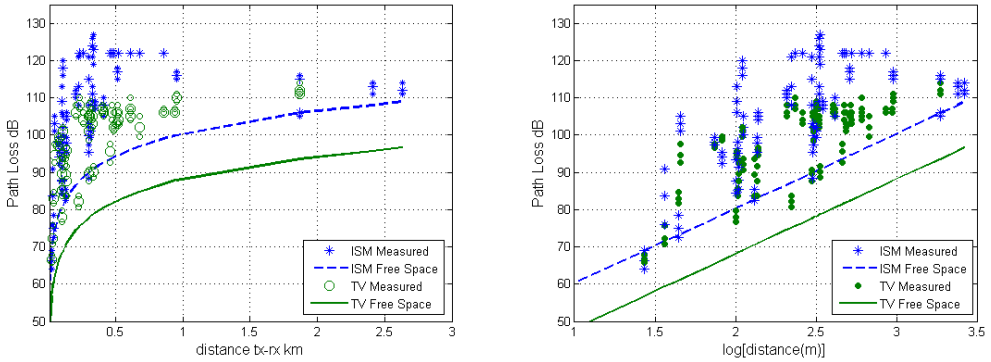

(a) Pathloss vs distance (b) Pathloss vs distance in log

Figure 5.3: ISM and TV band propagation loss

Loc	**ISM band**(dB)		**TV band**(dB)	
	Measured	Simulated	Measured	Simulated
1	-68.9...-62.9	-91...-83	-71.3...-66.3	-67...-63
2	-80.9...-65.9	-95...-87	-84.3...-80.3	-79...-71
3	-79.9...-74.9	-91...-83	-83.3...-77.3	-71...-63
4	-79.9...-76.9	-79...-71	-87.3...-85.3	-71...-63
5	-86.9...-84.9	-79...-71	x	-75...-67
6	x	-95...-91	-84.3...-81.3	-75...-71
7	-87.9...-82.9	-95...-91	-85.3...-83.3	-79...-75
8	x	-91...-87	-88.3...-85.3	-71...-67
9	-55.9...-49.9	>-59	-63.3...-60.3	>-55
10	-76.9...-74.9	-83...-79	-76.3...-75.3	-67...-63
11	-72.9...-69.9	-87...-79	-78.3...-77.3	-67...-63
14	-76.9...-72.9	-75...-67	-70.3...-62.3	-71...-63
15	x	<-95	-84.3...-80.3	-87...-83
16	x	≈-95	-86.3...-82.3	-87...-83
17	x	≈-95	-76.3...-71.3	-87...-83
18	x	x	-88.3...-84.3	-87...-83
19	x	<-95	-85.3...-82.3	-87...-79
20	x	<-95	-83.3...-78.3	-87...-79
21	x	x	-85.3...-84.3	-95...-87
22	x	-95...-87	-81.3...-79.3	-79...-75
23	x	x	-84.3...-81.3	-95...-87
24	-62.9...-59.9	-71...-63	-72.3...-62.3	-63...-59
25	-70.9...-61.9	-67...-63	-58.3...-55.3	-63...-59
26	-82.9...-77.9	-87...-83	-72.3...-69.3	-63...-59
27	-89.9...-87.9	-91...-87	-86.3...-83.3	-71...-63
28	-82.9...-78.9	-79...-71	-76.3...-71.3	>-55

Table 5.6: Measured vs simulated signal strength range Tx1

Loc	**ISM band**(dB)		**TV band**(dB)	
	Measured	Simulated	Measured	Simulated
29	-46.5...-41.5	>-59	-46.3...-44.3	>-55
30	-83.5...-82.5	-91...-83	-90.3...-89.3	-83...-79
31	-91.5...-88.5	-91...-87	x	-87...-79
32	-90.5...-86.5	-79...-71	-82.3...-80.3	-79...-75
33	x	-79...-71	-84.3...-82.3	-79...-75
34	-83.5...-81.5	-95...-91	-75.3...-73.3	-83...-79
35	-95.5...-92.5	-95...-91	-83.3...-81.3	-83...-79
36	-98.5...-85.5	-91...-83	-69.3...-66.3	-79...-75
37	-105...-96.5	-91...-83	-70.3...-67.3	-79...-75
38	-104...-98.5	<-95	-85.3...-82.3	-83...-79
39	-98.5...-85.5	-95...-87	-62.3...-59.3	-71...-67
40	-75.5...-72.5	-71...-67	-64.3...-62.3	-63...-59
41	x	<-95	-86.3...-84.3	-87...-83
42	x	<-95	-86.3...-83.3	-87...-83
43	-97.5...-93.5	-91...-83	-80.3...-78.3	-83...-75
44	-90.5...-83.5	-87...-83	-74.3...-72.3	-79...-75
45	-68.5...-53.5	-59...-55	-54.3...-49.3	>-55
46	-91.5...-88.5	-95...-91	x	-83...-79
47	-93.5...-92.5	-91...-87	-92.3...-90.3	-83...-79
48	x	-95...-91	-85.3...-84.3	-83...-79
49	-94.5...-92.5	<-95	-89.3...-87.3	-83...-79

Table 5.7: Measured vs simulated signal strength range Tx2

Loc	**ISM band**(dB)		**TV band**(dB)	
	Measured	Simulated	Measured	Simulated
1	-65.6	-87	-68.2	-65
2	-72.9	-91	-83.2	-75
3	-77.4	-87	-79.6	-67
4	-78.1	-75	-86.3	-67
5	-85.9	-75	x	-71
6	x	-93	-82.7	-73
7	-85.4	-93	-84.6	-77
8	x	-89	-86.8	-69
9	-52.7	>-59	-61.6	>-55
10	-75.8	-81	-75.5	-65
11	-71.7	-83	-77.9	-65
14	-75.4	-71	-66.3	-67
15	x	<-95	-80.8	-85
16	x	-95	-84.5	-85
17	x	-95	-74.2	-85
18	x	x	-86	-85
19	x	<-95	-83.1	-83
20	x	<-95	-81	-83
21	x	x	-84.8	-91
22	x	-91	-80.7	-77
23	x	x	-82.5	-91
24	-61.2	-67	-68.1	-61
25	-65.3	-65	-56.6	-61
26	-80.1	-85	-70.8	-61
27	-88.5	-89	-84.8	-67
28	-80.7	-75	-73	>-55

Table 5.8: Measured vs simulated mean signal strength Tx1

Loc	**ISM band**(dB)		**TV band**(dB)	
	Measured	Simulated	Measured	Simulated
29	-43.9	>-59	-45.1	>-55
30	-83.2	-87	-89.8	-81
31	-90.2	-89	x	-83
32	-88.9	-75	-81.7	-77
33	x	-75	-83.7	-77
34	-82.6	-93	-74.4	-81
35	-94.4	-93	-82	-81
36	-92.9	-87	-68.2	-77
37	-101	-87	-68.7	-77
38	-102	<-95	-83.8	-81
39	-90.3	-91	-60.6	-69
40	-73.8	-69	-63.7	-61
41	x	<-95	-85.3	-85
42	x	<-95	-84.7	-85
43	-95.4	-87	-79.3	-79
44	-86.5	-85	-73.1	-77
45	-61.3	-57	-50.9	>-55
46	-89.9	-93	x	-81
47	-92.5	-89	-90.9	-81
48	x	-93	-84.3	-81
49	-93.4	<-95	-88.5	-81

Table 5.9: Measured vs simulated mean signal strength Tx2

5.2.4 One slope model

Scatter plots of path loss versus distance in logarithm for both bands are given in figure 5.4 with 1 m reference distance. The best fit exponent value for ISM band is $n = 2.72$ with a standard deviation of 12.53 and for TV band is $n = 2.99$ with a standard deviation of 9.38.

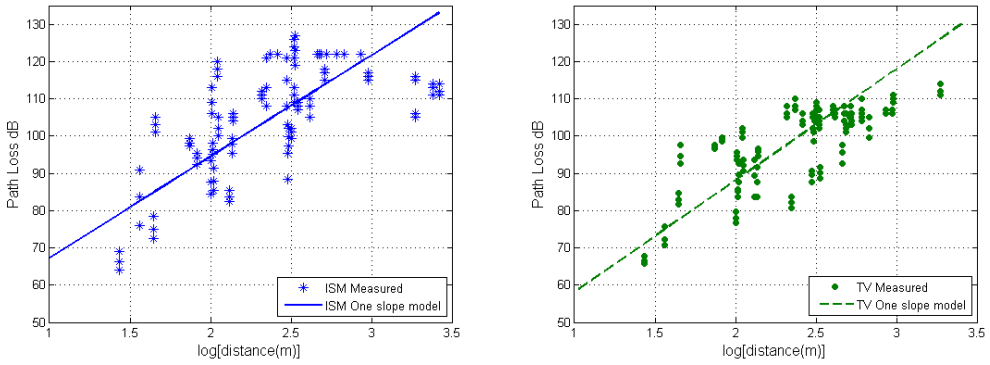

(a) ISM band (b) TV band

Figure 5.4: One slope path loss model

5.2.5 Okumura-Hata suburban model

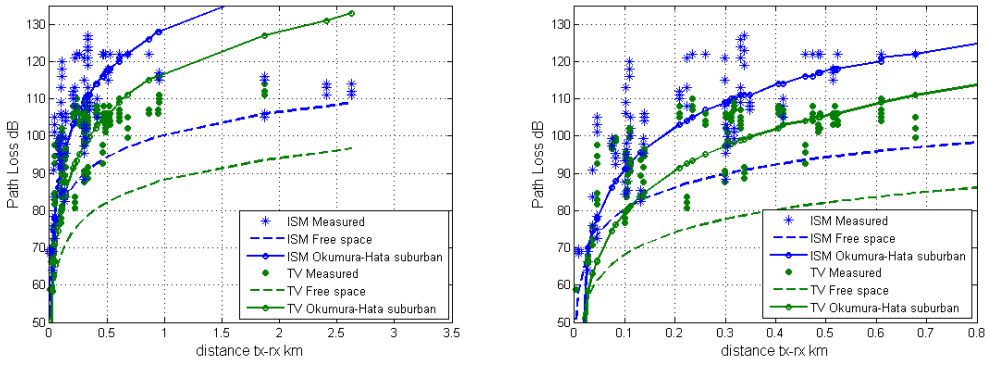

Figure 5.5: Okumura-Hata suburban propagation loss

The comparison result with Okumura-Hata suburban propagation model is shown in figure 5.5. As can be seen, beyond the distance of 1 km, an large excess propagation loss was expected in the Okumura-Hata model than free

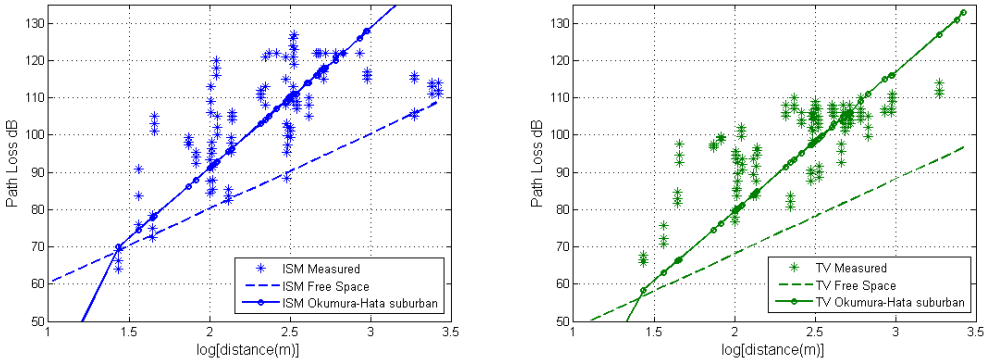

(a) ISM band (b) TV band

Figure 5.6: Okumura-Hata suburban propagation loss vs distance in log

space and the measured values. Additional attenuation was estimated in Okumura-Hata empirical model in this case. That might because in our measurement cases, the receivers at distance larger than 1.5 km were measured and only could be measured on the other side of the gulf and the signal propagation path to the receiver over the gulf could be considered as free space.

While within the distance of 1 km, as shown in figure 5.6(log(distance)¡3), the Okumura-Hata is no more over estimated the path loss. The predicted values could roughly match to the measured ones around 2.5 of log(distance). However, at the distance shorter than 100 m, the predicted value is smaller than the average measured path loss value. The transmitter height range used to get the Okumura-Hata empirical model was from 30 m to 1000 m. While in our measurement, the transmitter at the height is around 13 m, and even includes elevation data, the height is less than 25 meters. At the short distances, lowering the antenna height could result to less receivers in LOS locations and the attenuation caused by obstacles therefore would be increased. And due to the interference, the measured signal will be smaller than without the interference, as illustrated in section 5.3. The standard deviation error between the Okumura-Hata suburban model and mean measured path loss is 16.39 for ISM band and 14.50 for TV band.

5.2.6 COST 231 Hata model

Figure 5.7 shows the comparison results of measured path loss with free space propagation model and COST 231 Hata empirical propagation model and figure 5.8 shows the path loss vs the propagation distance in logarithm. As

can be seen in figure 5.7a, the model could not be used to predict ISM band propagation because it over estimated in most cases. While in TV band, as shown in figure 5.7b, at the distance shorter than 400 m, the predicted value are fairly meet the value of average path loss at corresponding distance. The standard deviation error between the Okumura-Hata suburban model and mean measured path loss is 19.94 for ISM band and 13.46 for TV band.

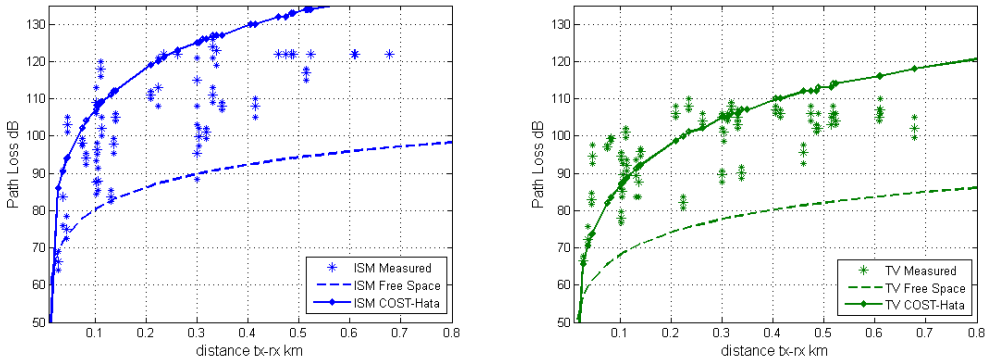

(a) ISM band (b) TV band

Figure 5.7: COST-Hata propagation loss

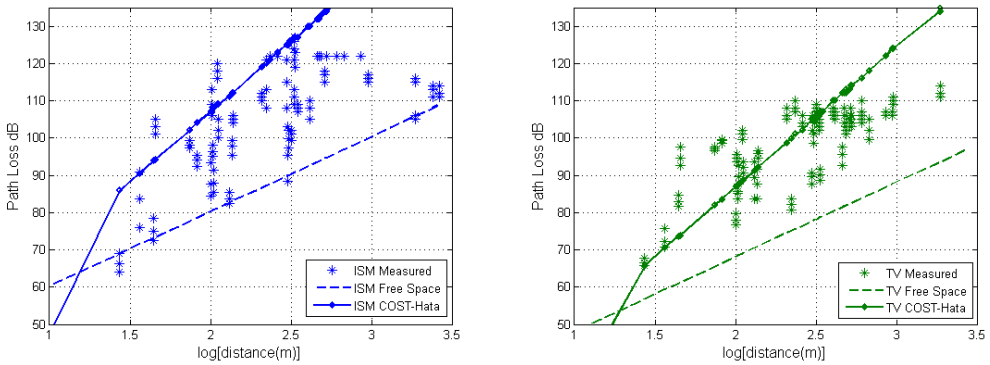

(a) ISM band (b) TV band

Figure 5.8: COST-Hata propagation loss vs distance in log

5.2.7 ITU-R P.1411 model

Plots of path loss derived from ITU-R P.1411 propagation model versus distance in logarithm with the measurement data from both bands are given in

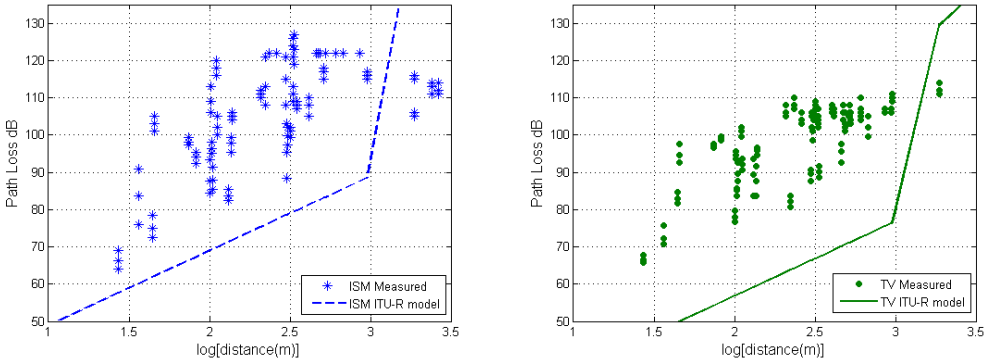

(a) ISM band (b) TV band

Figure 5.9: ITU-R P.1411 model path loss vs distance in logarithm

Empirical models	**standard deviation of error**	
	ISM band	**TV band**
Free space model	23.78	24.73
One slope model	12.53	9.38
Okumura-Hata model	16.39	14.50
COST-Hata model	19.94	13.46
ITU-R P.1411 model	36.31	33.55

Table 5.10: Standard deviation of error for each model

figure 5.9. The prediction curve goes around the measurement data in both bands and the error standard deviation is quite large: 36.31 for ISM band and 33.55 for TV band. The model was based on measurements made in the UHF band with antenna heights between 1.9 and 3.0 m above ground. Even the transmitter height in our case is near street level below roof-top height, but it still located at about 13 m high place. A correction factor should be derived if this model is adopted.

5.2.8 Comparison of standard deviation for each model

The standard deviation of error for each model are shown in table 5.10. As can be seen, the One slope propagation model gives the best fit to the measurement data both in ISM band and TV band. The COST-Hata model is the second suitable propagation model for TV band signals, which shows smaller standard deviation of error than Okumura-Hata model. However from the comparison between figure 5.5 and figure 5.7, it can be seen that

when the transmission distance between transmitter and receiver beyond 500 m, the COST-Hata model will have more excess deviation than other models and the performance of the prediction will down grade rapidly.

5.3 Calibration

As mentioned in Section 5.2.1, the measurement at some locations showed strange situations that a calibration was implemented in laboratory to find the reasons. In this section, the calibration set-up and measurement details in the laboratory would be introduced.

5.3.1 Set up in laboratory

The calibration setup used in the laboratory is shown in figure 5.10. The receiver configuration for TV band is the same as TV band receiver 2 without the antenna part. Transmitter and receiver were located as far as possible from each other via long cable that the Dlink transmitter does not leak directly via air to Dlink receiver and set the received signal level. In transmitter end the variable attenuator (0-110 dB) was set to 70 dB that the receiver could be close to its sensitivity level and receiver end variable attenuator (0-11 dB) fine-tuned the level.

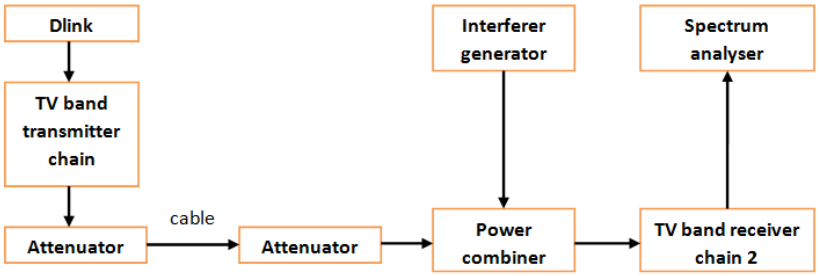

Figure 5.10: Laboratory calibration set up

QPSK modulated interferer (8 MSPS) was generated by interferer generator. The 99% bandwidth is about 10 MHz, see figure 5.11. The interference level was set by the generator. We did not have DVB-T signal, which is used in TV transmissions, but this set-up should not cause big differences to the results.

TV band wanted signal and interferer were summed by a power combiner. After that is the reference antenna connector point (in real field measurement

the point after the receiver antenna and antenna cable). Therefore interferer level has to be scaled by -4 dB with respect to generator value (generator cable loss and power combiner loss) and wanted signal has to be scaled by -12 dB with respect to Dlink received signal value (converter gain reduced away because Dlink received signal strength reference point is its input). These scaling are made directly to the results and the original results are not shown.

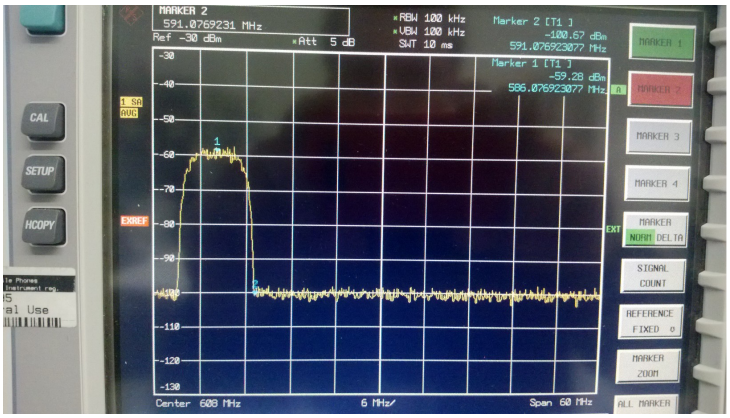

Figure 5.11: Interference

5.3.2 Calibration measurement

5.3.2.1 The wanted signal only

The wanted signal is set to 618 MHz (607-629 MHz). In the table 5.11 are listed measured received signal strength values as a function of relative wanted signal to the sensitivity level.

As can be seen the received signal strength levels follow quite linearly at higher signal levels the input signal strength changes. At lower levels it starts to saturate and variation in received signal strength level becomes wider. There might be two reasons for that, 1) received signal strength is most probably measuring in DLINK power and receiver noise starts to affect at lower levels to the result and 2) Dlink received signal strength measurement as itself becomes more inaccurate at lower levels. As a reference noise level at the receiver reference point is -174 dBm/Hz + 10*log10(BW) + NF = -101 + NF.

The next test was that when the wanted signal is set to its sensitivity level (SENS), what the allowed interferer level is so that the wanted signal can be detected. The interferer frequency was set to 586 MHz. As the result, the

Input signal over sensitivity level x dB	**Received signal strength/dBm**
0	-97 . . . -93
3	-95 . . . -92
6	-93 . . . -92
10	-91 . . . -90
16	-87 . . . -86
26	-77 . . . -76
36	-68 . . . -67

Table 5.11: Measured signal level with respect to input signal

maximum interferer level is -70 dBm that can ensure the wanted signal at its sensitivity level could be detected. When comparing to the real TV signal interferer measured this is about 20 dB smaller than in real environment. That is the reason why we were not able to measure our test signal in TV band at its sensitivity level except in very rear cases.

Kivenlahti TV station is sending 'kanavanippu' D at the frequency of 586 MHz using ERP of 35 kW. The height of the Kivenlahti TV station tower from the sea level is 326 m. The signal level at OIH using only FSL (Free Space Loss) equation is about -32 dBm. This is about 18 dB larger than the measured value. The reasons for that may be shadowing and the TX antenna radiation pattern.

5.3.2.2 Interference measurement

The following measurements show the effect of interferer to the wanted signal in four cases:

1. Set the interferer at 586 MHz and the wanted signal fixed, interferer level varied, measure received signal strength value;

2. Set the wanted signal level fixed, interferer from 586 MHz towards the wanted signal varying the level, measure the received signal strength value;

3. Set the interferer at 586 MHz, wanted signal in different levels with 2 options (normal measurement setup and 10 dB attenuator after the LNA), interferer level varied, measure the received signal strength value.

Input signal over sensitivity level x dB	$P_{interferer}$ dBm	**Received signal strength** dBm	**Note**
16	-43	-97 . . . -91	≈ -87 no interference
16	-49	-97 . . . -80	
16	-55	-91 . . . -89	
16	-58	-89 . . . -87	
16	-61	-87 . . . -86	

Table 5.12: Case 1 result

Note that when the interferer is about -50 dBm or less, then those values are relevant to our field measurement results. Also in cases 1-3 the $P_{interferer}$ is given only in the input of DUT (Device Under Test) and to make them comparable to RSSI value they have to be scaled up by 12 dB.

Case 1 results are shown in the table 5.12. It seems that there is a tendency of having the smaller received signal strength values the higher the interference is.

Case 2 results are shown in the table 5.13. The input signal (x+SENS) was set to 10 dBm. As can be seen in the table, the tolerance interference level is getting smaller when towards the wanted signal band.

Case 3 results are shown in the table 5.14. The wanted input signal RSSI value was measured without interference at 3 different levels: 1) sensitivity limit (SENS) for normal setup and with extra attenuator after LNA; 2) SENS + 16 dB (SENS is the value of normal setup) and 3) SENS + 26 dB. Note that in all cases the results are shown after RF front end gain compensation to the measured RSSI values. Therefore for example in SENS measurement in the limit the RSSI value was the same in both cases.

Next the wanted input signal RSSI value was measured with interfering signal (f=586 MHz, BW = 8 MHz) at two wanted signal levels (SENS+16 dB, SENS+26 dB) as a function of interfering signal levels.

The wanted input signal levels in each case: SENS+26 dB = -75 dBm, SENS+16 dB = -85 dBm, SENS (normal setup) = (-101 dBm -SENS (extra attenuator)) = -91 dBm.

When the wanted input signal (normal setup) is SENS + 16 dB, in normal setup the limit of operation is reached at $P_{interferer}$ = -34 dBm in Dlink input (51 dB higher than the wanted signal). While in the extra attenuator setup

$F_{interference}$ **MHz**	$P_{interferer}$ dBm	**Received signal strength** dBm	**Note**
-	-	≈ -91	No interference
600	-55	-81 . . . -78	
600	-60	-93 . . . -90	
601	-60	-79 . . . -78, -92 . . . -90	RSSI values concentrated into 2 range blocks
601	-64	-92 . . . -91	
602	-64	-79 . . . -77, -92 . . . -90	RSSI values concentrated into 2 range blocks
602	-66	-91 . . . -90	
603	-63	-75 . . . -73, -90 . . . -86	RSSI values concentrated into 2 range blocks
603	-66	-90 . . . -85	
604	-51	-70 . . . -66	
604	-63	-83 . . . -70	
618	-88	-90 . . . -86	
618	-94	-91 . . . -89	

Table 5.13: Case 2 result

Input signal over sensitivity level x dB	$P_{interferer}$ dBm in DUT (input of Dlink normal case/with extra attenuator)	**Received signal strength** dBm (normal setup)	**Received signal strength** dBm (10 dB attenuator after LNA)	**Note**
0	-	-94 ...-92	-85 ...-82	Normal setup SENS setting is used as reference
16	-	-85 ...-84	-83 ...-81	
16	-70 (-58/-68)	-86 ...-83	-83 ...-81	
16	-60 (-48/-58)	-86 ...-84	-83 ...-81	
16	-56 (-44/-54)	-88 ...-85	-83 ...-81	
16	-54 (-42/-52)	-89 ...-87	-83 ...-81	
16	-51 (-39/-49)	-93 ...-91	-83 ...-82	
16	-49 (-37/-47)	-95 ...-92	-84 ...-82	
16	-46 (-34/-44)	-94 ...-78	-86 ...-83	Limit for normal setup
16	-44 (-32/-42)	-	-87 ...-84	Limit for extra attenuator in RX path
26	-	-76 ...-74	-76 ...-73	
26	-70 (-58/-68)	-76 ...-74	-76 ...-73	
26	-60 (-48/-58)	-76 ...-74	-76 ...-73	
26	-54 (-42/-52)	-79 ...-77	-75 ...-73	
26	-51 (-39/-49)	-80 ...-79	-76 ...-74	
26	-49 (-37/-47)	-87 ...-85	-76 ...-74	
26	-46 (-34/-44)	-89 ...-86	-78 ...-76	
26	-44 (-32/-42)	-90 ...-87	-79 ...-77	
26	-42 (-30/-40)	-94 ...-84	-81 ...-79	
26	-40 (-28/-38)	-93 ...-80	-84 ...-80	Limit for normal setup
26	-38 (-26/-36)	-	-84 ...-82	
26	-36 (-24/-34)	-	-84 ...-76	
26	-34 (-22/-32)	-	-84 ...-76	Limit for extra attenuator in RX path

Table 5.14: Case 3 result

the limit of operation is reached at $P_{interferer}$ = -42 dBm in Dlink input (43 dB higher than the wanted signal)

When the wanted input signal (normal setup) is SENS + 26 dB, in normal setup the limit of operation is reached at $P_{interferer}$ = -28 dBm in Dlink input (47 dB higher than the wanted signal). While in extra attenuator setup the limit of operation is reached at $P_{interferer}$ = -32 dBm in Dlink input (43 dB higher than the wanted signal).

The normal setup have better interference performance at the input of Dlink, but in real measurement environment, where the situation is looked at the antenna connector, the performance with extra attenuator is better in cases of the wanted input is well above the signal the sensitivity level. Before breaking the operation the RSSI value is increased with respect the case without any interferer. The reason for that might be that RSSI measures the total power, but to detect the wanted signal a signal spreading of beacon improves decoding of bits until the limit has been reached. In case of a high power interferer signal near the wanted signal the receiver with extra attenuator is better than the normal setup. The cost of that is a clear degradation in measuring of very low level wanted signals (without any high power interferer signal near the wanted signal). For TV band extra RF module before the Dlink was needed to convert the signal from TV band to ISM band. The front end gain is a compromise between the tolerance to interference and ability to measure very weak signals.

Chapter 6

Conclusion

This chapter the implications of results deduced from the measurement data are discussed. The directions in which the current work could be extended are also presented in the end of the work.

6.1 Summary

This thesis deals with the outdoor signal strength measurement in Otaniemi campus area for the purposes of comparing the propagation characteristics of TV band and ISM band. The measurement setup designed for outdoor measurement, including the transmitter, the receiver, the antenna, the signal source and the measurement equipments is given in details and then the measurement scenario, data collection method and a coverage simulation result are presented in brief.

The results got from the measurement were processed and displayed in a path loss versus distance distribution diagram and were compared to the predicted values derived from various empirical propagation models. When comparing the measured path loss results to the different propagation models, the free space model under-estimates the propagation loss at both bands with different deviation to the measured path loss. While in the far field beyond 1 km to the transmitter, the deviation to the ISM band measured value is getting smaller. The Okumura-Hata suburban model shows the best agreement at ISM band in the near field within 800 m, while it under-estimates the TV band propagation in the distance shorter than 300 m and over-estimates in the distance larger than 500 m. The one slope propagation model in general is the most suitable empirical model with standard deviation of the errors at 12.53 for ISM band and 9.38 for TV band.

We can also notice a high variance of path loss at the locations very close

to each other. This is caused probably by the multipath effect and lognormal shadowing caused by high density of buildings and trees. However, this fact implies the difficulties in usability of such measurement for the distance estimation. when the different building heights, spacing and construction methods are taken into account, along with the attenuation due to trees, the resultant distribution function is very close to lognormal [45]. Although received values are decreasing with the distance, their variance causes that the measured value cannot be used for the distance determination with certainty.

In some locations the TV band signals were expected while nothing could be detected. A calibration was conducted in laboratory to deal with these phenomena. A interference TV signal was detected. The interfering TV signal is a large coverage interferer, which may effect on measurement results in many cases. From the calibration measurement results it seems that if the TV interferer is less than -58 dBm in antenna connector, then it has no effect on results. Around -50 dBm it causes received signal strength values which are somewhat lower than the real value with no interferer. Based on interference calibration measurements in a laboratory a good compromise between the tolerance to a high level nearby interferer and ability to measure weak wanted signal would have been the designed RF front-end structure to TV band with gain of about 6 dB instead of 12 dB (an addition of a 6 dB attenuator e.g. before the mixer).

6.2 Future work

Finally, we explore different directions in which the current research work could be extended. In this thesis, we got the measured results in outdoor scenarios. It would be interesting to study the propagation characteristics in indoor scenario with the same transmitter and receiver set up. The results presented in the thesis are limited to the sensitivity capability and accuracy of the measurement equipment - Dlink box. In the indoor measurement, laboratory measurement equipment which is not heavy and unsuitable for outdoor measurement but with higher sensitivity level and accuracy could be used. And it would be interesting to have a comparison of the results got from different equipments.

It would also be interesting to continue the outdoor measurement by putting the transmitter to a higher place, eg. the roof top of OIH building, to reduce the multipath effect caused by buildings and trees. Since the Kivenlahti TV signal is sending at the frequency of 586 MHz and the TV test band license is valid for the band 590 - 630 MHz. To minimize the effect of interference the measured TV band could be set only to 618 MHz and a

frequency trap built to the TV signal frequency with a compensating reactance to minimize the effect on the test signal. This frequency trap should be located to the TV band receiver filter before the mixer from the TV band to ISM band.

Bibliography

[1] T. Baykas, M. Kasslin, M. Cummings, H. Kang, J. Kwak, R. Paine, A. Reznik, R. Saeed, and S. J. Shellhanner, "Developing a standard for tv white space coexistence: Technical challenges and solution approaches," *IEEE Wireless Communications*, vol. 19, pp. 10–22, 2012.

[2] OpenWRT, "D-link dir-825," 2012. Available:`http://wiki.openwrt.org/toh/d-link/dir-825`.

[3] Cisco, "Cisco visual networking index: Global mobile data traffic forecast update, 2011-2016," 2012. `http://www.cisco.com/en/US/solutions/collateral/ns341/ns525/ns537/ns705/ns827/white_paper_c11-520862.html`.

[4] T. Renk, V. Blaschke, and F. K. Jondral, "Time-dependent statistical analysis of measurements for the evaluation of vacant spectrum bands," *URSI General Assembly*, 2008. Chicago, Illinois. Available: `http://www.ursi.org/proceedings/procGA08/papers/C08p1.pdf`.

[5] I. F. Akyildiz, W.-Y. Lee, M. C. V. *, and S. Mohanty, "Next generation/dynamic spectrum access/cognitive radio wireless networks: A survey," *Computer Networks (50)*, pp. 2127–2159, 2006. Available: `http://www.ece.gatech.edu/research/labs/bwn/surveys/radio.pdf`.

[6] M. H. Islam, C. L. Koh, S. W. Oh, X. Qing, Y. Y. Lai, C. Wang, Y.-C. Liang, B. E. Toh, F. Chin, G. L. Tan, and W. Toh, "Spectrum survey in singapore: Occupancy measurements and analyses," *3rd International Conference on Cognitive Radio Oriented Wireless Networks and Communications*, pp. 1–7, 2008.

[7] FCC, "Report of the spectrum efficiency working group, et docket no.02-155," 2002.

[8] R. Thanki, "The economic value generated by current and future allocations of unlicensed spectrum," 2009.

[9] K. Ruttik, "Secondary spectrum usage in tv white space," 2011.

[10] J. van de Beek, J. Riihijärvi, A. Achtzehn, and P. Mähönen, "Uhf white space in europe - a quantitative study into the potential of the 470-790 mhz band," *IEEE International Symposium on Dynamic Spectrum Access Networks*, 2011.

[11] DigitalUK, "Tv regions." Available:`www.digitaluk.co.uk/when_do_i_switch`.

[12] E. I. Society, "Finland." Available:`http://ec.europa.eu/information_society/policy/ecomm/doc/implementation_enforcement/annualreports/14threport/fi.pdf`.

[13] H. T. FRIIS, "A note on a simple transmission formula," 1946.

[14] M. J. Marcus, "Unlicensed cognitive sharing of tv spectrum: the controversy at the federal communications commission," *Communications Magazine, IEEE*, vol. 43, pp. 24–25, 2005.

[15] P. Bahl, R. Chandra, T. Moscibroda, R. Murty, and M. Welsh, "White space networking with wi-fi like connectivity," *SIGCOMM '09 Proceedings of the ACM SIGCOMM 2009 conference on Data communication*, vol. 39, pp. 27–38, 2009. Available: `http://dl.acm.org/citation.cfm?id=1592573`.

[16] K. Andersson, "Super wi-fi: Using tv white spaces for rural broadband," 2011. Available: `http://www.carlsonwireless.com/products/brochures/White_Spaces_White_Paper.pdf`.

[17] Neul, "Neul launches world's first city-wide white space network," 2012. Available: `http://www.neul.com/neul-pr-250412.php`.

[18] R. A.Saeed and S. J.Shellhammer, "Tv white space use cases," 2011.

[19] P. Marshall, "Xg communications program information briefing," 2005. Available: `http://www.daml.org/meetings/2005/04/pi/DARPA_XG.pdf`.

[20] FCC, "Second report and order and memorandum opinion and order in et docket nos. 02-380 (additional spectrum for unlicensed devices below 900 mhz and in the 3 ghz band) and 04-186 (unlicensed operation in the tv broadcast bands)," 2008. Available: `http://hraunfoss.fcc.gov/edocs_public/attachmatch/FCC-08-260A1.doc`.

[21] Ofcom, "Digital dividend: cognitive access statement on license-exempting cognitive devices using interleaved spectrum," 2009. Available: http://www.ofcom.org.uk/consult/condocs/cognitive/statement/statement.pdf.

[22] M. of Transport and Communications, "Testing of cognitive radio systems possible," 2009. Available: http://www.lvm.fi/web/en/pressreleases/-/view/1043567.

[23] RSPG, "Opinion on cognitive technologies, rspg10-348 final," 2011. Available: http://rspg.ec.europa.eu/_documents/documents/meeting/rspg24/rspg_10_348_ct_opinion_final.pdf.

[24] ECC, "Technical and operational requirements for the possible operation of cognitive radio systems in the 'white space' of the frequency band 470-790 mhz, ecc report 159," 2011. Available: http://www.erodocdb.dk/docs/doc98/official/Pdf/ECCRep159.pdf.

[25] Adaptrum, "Adaptrum supplies tv whitespace solution to uk cambridge tv white spaces trial," 2011. Available: http://www.adaptrum.com/.

[26] IDA, "Trial of white space technology accessing vhf and uhf bands in singapore," 2010.

[27] Microsoft, "Microsoft research whitefi service," 2010. Available: http://whitespaces.msresearch.us/.

[28] I. Canada, "Smse-012-11: Consultation on a policy and technical framework for the use of non-broadcasting applications in the television broadcasting bands below 698 mhz," 2011.

[29] I. . R. R. T. A. Group, "Response to the industry canada consultation on a policy and technical framework for the use of non-broadcasting applications in the television broadcasting bands below 698 mhz," 2011. Available: https://mentor.ieee.org/802.18/dcn/11/18-11-0075-04-0000-ieee-802-response-to-canadian-tvws-consultation.doc.

[30] IEEE802.11af, "Ieee standard for information technology telecommunications and information exchange between systems local and metropolitan area networks specific requirements ? part 11: Wireless lan medium access control (mac) and physical layer (phy) specifications," 2011. Available: http://www.ieee802.org/11/Reports/tgaf_update.htm.

[31] IEEE802.15.4, "Project authorization request for ieee standard for local and metropolitan area networks part 15.4: Low rate wireless personal area networks (lr-wpans) amendment: Tv white space between 54 mhz and 862 mhz physical layer," 2011.

[32] ETSI, "Tc rrs activity report 2009," 2009. Available: `http://portal.etsi.org/rrs/activityreport2009.asp`.

[33] T. K.Sarka, Z. Ji, K. Kim, A. Medouri, and M. Salazar-Palma, "A survey of various propagation models for mobile communication," *IEEE Antenna and Propagation Magazine*, vol. 45, 2003.

[34] J.D.Parsons, "The mobile radio propagation channel:2nd edition," 2000.

[35] Y. Okumura, E.Ohmori, T.Kawano, and K.Fukuda, "Field strength and its variability in vhf and uhf land mobile radio service," *Review of the Electrical Communications Laboratory*, vol. 16, pp. 825 – 873, 1968.

[36] M. Hata, "Empirical formula for propagation loss in land mobile radio services," *IEEE Transactions on Vehicular Technology*, vol. 29, pp. 317 – 325, 1980.

[37] C. A. 231, "Digital mobile radio towards future generation systems final report," 1999.

[38] ITU-R, "Recommendation itu-r p.529-3, prediction methods for the terrestrial land mobile service in the vhf and uhf bands," 1999.

[39] ITU-R, "Recommendation itu-r p.370-7, vhf and uhf propagation curves for the frequency range from 30 mhz to 1000 mhz broadcasting services," 1995.

[40] ITU-R, "Recommendation itu-r p.1546-4, method for point-to-area predictions for terrestrial services in the frequency range 30 mhz to 3000 mhz," 2009.

[41] ITU-R, "Recommendation itu-r p.1146, the prediction of field strength for land mobile and terrestrial broadcasting services in the frequency range from 1 to 3 ghz," 1995.

[42] ITU-R, "Recommendation itu-r p.1411-6, propagation data and prediction methods for the planning of short-range outdoor radiocommunication systems and radio local area networks in the frequency range 300 mhz to 100 ghz," 2012.

[43] R. Passini and K. Jacobsen, "Accuracy analysis of srtm height models," 2007.

[44] M. A. Weissberger, "An initial critical summary of models for predicting the attenuation of radio waves by foliage," 1982. ESD-TR-81-101.

[45] S. Saunders and A. Aragon-Zavala, "Chapter 9: Shadowing," 2007.

[46] R. Ahola, "Integrated radio frequency synthesizers for wireless applications," 2005.

Appendices

Appendix A

Components of transmitter and receivers

In this appendix, the details of components in the transmitter and receiver architecture including the component function, the component model used and the corresponding important parameters are introduced.

A.1 Diplexer

Diplexer is a passive component that can be used to enable different devices to share a common communications channel. So diplexer might be used to connect more than one transmitter to a single transmitting antenna and also it can connect more than one receiver to a same receiving antenna. The transmitters/receivers usually operate on different frequencies and diplexer will be placed between the transmitters/receivers and antenna.

The diplexer model we used here is RDP-272+ which combined of low pass and high pass filters and consists of three ports: a common port, a low pass port and a high pass port, as showed in the functional schematic figure A.1, low pass port and high pass port are multiplexed to common port. In this way, the diplexer routes all the signals at frequencies below 950 MHz to low pass port and the signals between 1700 MHz and 2700 MHz to high pass port. The insertion loss is very low, about 0.4 dB for 600 MHz TV band and 0.56 dB for 2.4 GHz ISM band. The level of isolation is very high, typically 48 dB for low pass stop band frequency at 1700 - 2700 MHz and 35 dB for high pass stop band frequency below 950 MHz, which means negligible low band signal will be transferred from the common port to the high pass port and vice versa.

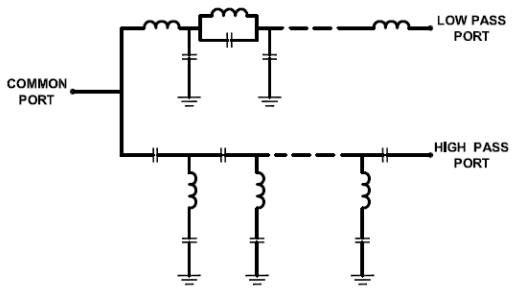

Figure A.1: Diplexer functional schematic

A.2 Amplifier

Amplifier is a device for increasing the power of a signal by use of an external energy source. Low-noise amplifier (LNA) is an electronic amplifier used to amplify possibly very weak signals to acceptable levels with minimum self-generated additional noise. It is usually placed very close to the detection device to reduce losses in the feedline. When using LNA, noise is reduced by the gain of the amplifier while the noise of the amplifier is injected directly into the received signal. So LNA is required to boost the desired signal power while adding as little noise and distortion as possible.

ZHL-3010+ mini circuit model amplifier was used for TV band transmitter. It operates on wideband from 50 to 1000 MHz with low noise figure, typically 5.5 dB and high IP3, 46 dBm. IP3 refers to third order intercept point. It is the point where the amplitude of third order inter modulation is equal to the that of fundamental. In logarithm scale, a third-order nonlinear product will increase by 3 dB in power when the input power is raised by 1 dB. ZRL-3500+ model was used for ISM band transmitter with 2.5 dB noise figure and 44 dBm IP3. The operating frequency band is 700 to 3500 MHz. At the receiver end, ZX60-33LN+ and ZX60-43-S+ models were used after diplexer and synthesizer as LNA and buffer amplifier, respectively. The frequency range of ZX60-33LN+ LNA is 50 to 3000 MHz with 1.1 dB noise figure and 32.5 dBm IP3. ZX60-43-S+ model operates in the frequency range of 0.5 to 4000 MHz with 5.5 dB noise figure at frequency 3000 MHz and IP3 is 32 dBm. All the parameters are listed in the table A.1.

Mini circuit model	**Location**	**Frequency band (MHz)**	**NF (dB)**	**IP3 (dBm)**
ZHL-3010+	TV band Tx	50 - 1000	5.5	46
ZRL-3500+	ISM band Tx	700 - 3500	2.5	44
ZX60-33LN+	TV band Rx after diplexer	50 - 3000	1.1	32.5
ZX60-43-S+	TV band Rx after synthesizer	0.5 - 4000	5.5	32

Table A.1: Amplifier models and parameters

A.3 Attenuator

Attenuator is an passive electronic device that can reduce the amplitude or power of signal without appreciably distorting its waveform which is the opposite of an amplifier. An amplifier provides gain, an attenuator provides loss, or gain less than 1. Attenuator is used to protect the device from signal levels that might damage it and to match impedances by lowering apparent standing wave ratio. The attenuator should be in high accuracy. A typical T-pad attenuator is showed in figure A.2.

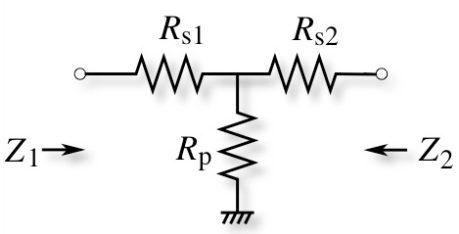

Figure A.2: Attenuator

A.4 Filter

Filter performs an important role in both transmitter and receiver design, especially in the TV band transfer system, which specifically to remove unwanted frequency components from the signal and to enhance the wanted ones. In the transmitter, we used low pass filter in the 600 MHz system and band pass filter in the 2.4 GHz system. In the receiver, both low pass filter

and band pass filter are used in the TV band system while no filter is used in the ISM band receiver.

A.4.1 Low pass filter

A low-pass filter is an electronic filter that passes low-frequency signals and attenuates signals with frequencies higher than the cutoff frequency. A basic electrical schematic is showed in Figure A.3. VLF-630 mini circuit model was used in the 600 MHz TV band transmitter and receiver. The typical frequency attenuation is showed in Figure A.4 where we can see that the pass band which attenuation is smaller than 1 dB is the frequency below 630 MHz and when the frequency is between 1000 and 6000 MHz, the attenuation will be very high, larger than 20 dB. Consequently, the signals in the ISM band could be well filtered by this low pass filter.

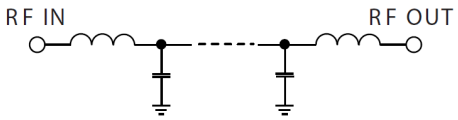

Figure A.3: Low pass filter electrical schematic

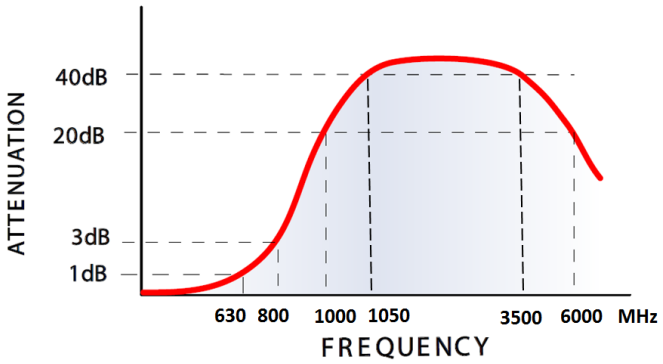

Figure A.4: Low pass filter frequency attenuation

A.4.2 Bandpass filter

A band-pass filter is a device that passes frequencies within a certain range and rejects frequencies outside that range. A basic electrical schematic is

showed in Figure A.5. The band pass filter model ZFBP-2400+ was used in our case. The lower stop band is frequency lower than 1800 MHz and 2800 MHz is the upper stop band.The typical rejection could be as high as 50 dB and the typical VSWR is 1.3:1 in the pass band.

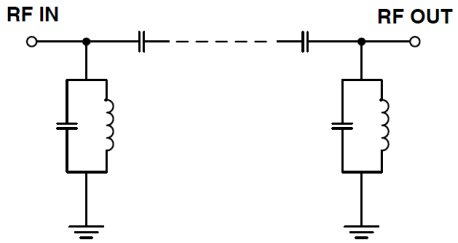

Figure A.5: Band pass filter electrical schematic

A.5 Frequency mixer

Frequency mixer is a nonlinear electronic component that can convert signal at one frequency to another frequency. The second frequency is either higher which is called frequency up-conversion for the mixing process, or lower, which is called frequency down-conversion. As in figure A.6, mixer consists of three ports, two input ports and an output port. These ports are all identified separately as each one has different characteristics. The signal input at frequency $f1$ that will be converted in frequency domain and the other input is typically connected to the local oscillator which generates a certain frequency $f2$. The output will be $f_1 \pm f_2$.

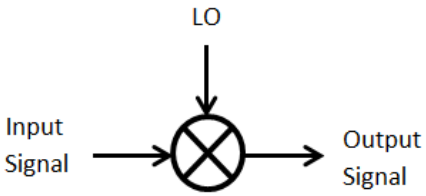

Figure A.6: Mixer

At transmitter end frequency mixer model ZX05-U742MH+ was used which converted 2.4 GHz frequency to 600 MHz frequency for transmission.

The typical conversion loss was 8.3 dB and third-order intercept point was 20 dBm typically.

The frequency mixer model we used in receiver was ZEM-4300+ which operated as up converter mixer that converted 600 MHz intermediate frequency to 2.4 GHz for DLink to receive. The synthesizer acts as LO and generate a frequency at 3000 MHz. This mixer has low conversion loss which is typically 6.65 dB.

A.6 Frequency synthesizer

Frequency synthesizer is an electronic system that can generate a range of frequencies from a single fixed oscillator. Two types of synthesizer can be distinguished based on feed back action, namely direct synthesis and indirect synthesis. 'Indirect' refers to a system based on a feedback action, whereas 'direct' refers to a system having no feedback [46]. The phase lock loop (PLL) and oscillator are playing important roles in frequency synthesizer.

We use 5008 dual frequency synthesizer module developed by Valon Technology[1] here and the output frequency range is 137.5 to 4400 MHz. It consists of two integer/fractional-N synthesizer chips and both synthesizers are referenced to a common 10 MHz temperature stabilized crystal oscillator (TCXO), as showed in figure A.7. A software controlled switch also lets the user select an external reference which should be an integer multiple of 10 MHz.

Both synthesizer will operate either in the fractional-N or integer-N mode depending on the user selected frequency. The integer-N synthesizer divide the output frequency by an integer number to produce the phase comparison frequency. Consequently, the output frequency can only be an integer multiple of the phase comparison frequency. In the fractional-N synthesizer, the divisor N is switched between two or more integer values in such a way that the average value of N can be a fractional number. As a result, the phase comparison frequency can be much higher than in integer-N synthesizers, and thus the division ratio can be much lower. It also brings disadvantages which have been discussed in [46]. As for our case, the synthesizer will be operating in the factional-N mode whenever a channel frequency is not an integer multiple of 10 MHz is selected.

The USB serial interface and the configuration manager software allows the user to program the desired operating frequency of each synthesizer and save to the on-board FLASH memory which retains the setting after power

[1] `http://valontechnology.com/`

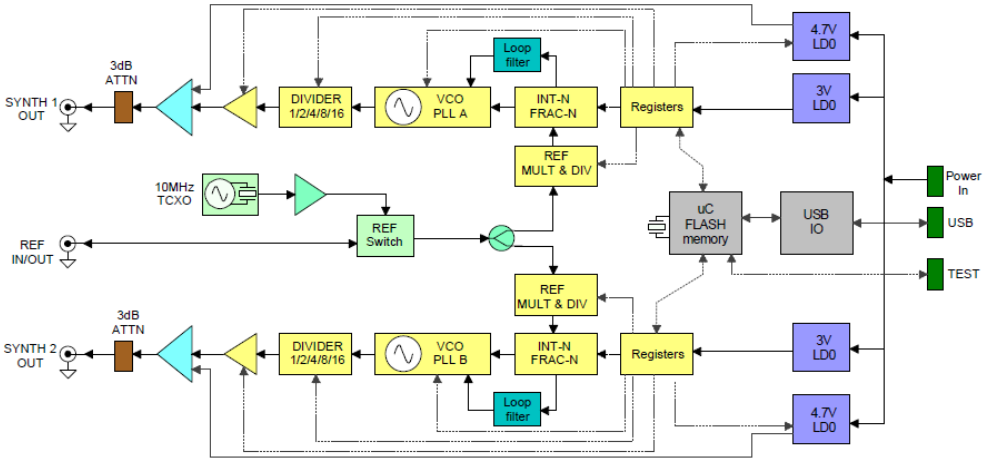

Figure A.7: Synthesizer block diagram

down.

Appendix B

OpenWrt

B.1 Introduction

OpenWrt is a Linux distribution for embedded devices. It provides a fully writable filesystem with package management 'opkg' and all components have been optimized for size, to be small enough to fit the limited available storage and memory. The applications can be selected and configured based on developers' own needs. There is no need to build a complete firmware around OpenWrt.

B.2 Configuration

In this section, the main configuration steps of transmitter and receiver will be introduced.

B.2.1 Transmitter configuration

Assume the OpenWrt system was already flashed using firmware recovery mode in the Dlink box and necessary packages were installed and configured.

- First using 'ssh' to login the OpenWrt system.

  ```
  sudo ssh root@192.168.0.76
  ```

- Pass word would be asked and just type in the right one.
- Modify the time zone to utc time

  ```
  date -u
  ```

The time can also be set manually by the command below, but in this way, deviation would be introduced between transmitter and receiver.

```
date -s hh:mm[:ss]
or date -s [YYYY.]MM.DD-hh:mm[:ss]
or date -s YYYY-MM-DD hh:mm[:ss]
or date -s [[[[[YY]YY]MM]DD]hh]mm[.ss]
```

- Configure the network and wireless files in /etc/config/, as showed in section B.3 but pay attention that here is transmitter, so the 'option mode' in 'wifi-iface' should be set in 'ap' mode. Check the beacon intervals, operation channel and working bandwidth.
- Turn on wifi.

```
ifconfig wlan0 up
wifi up
```

B.2.2 Receiver configuration

Assume the OpenWrt system was already flashed using firmware recovery mode in the Dlink box and necessary packages were installed and configured. First several steps are same as transmitter configuration.

- Using 'ssh' to login OpenWrt system.
- Modify the time zone to utc time.
- Configure the network and wireless files in /etc/config/, as showed in section B.3. Pay attention to the operation channel and working bandwidth.
- Mount usb to store the captured data.

```
mount -t ext4 /dev/sda /mnt/shares -o rw,sync
```

- Add a monitor interface to capture PHY packet RSSI.

```
iw phy0 interface add mon0 type monitor
ifconfig mon0 up
```

- Scan the available access points and find the wanted transmitter.

```
iwlist scan
```

- Create a connection to the transmitter access point.

```
iw wlan0 connect 'ssid'
```

- Check the connection.

```
iw wlan0 link
```

- If there is no connection created, kill the wpa process and try again.

```
killall -9 wpa_supplicant
```

- Start capturing using 'tcpdump'.

B.3 OpenWrt configuration files

B.3.1 Wireless configuration

```
#/etc/config/wireless Rx

config wifi-device  radio0
option type     mac80211
option channel  11
option macaddr 00:26:5a:f4:17:3d
option hwmode 11ng
option htmode HT20
list ht_capab SHORT-GI-40
list ht_capab TX-STBC
list ht_capab RX-STBC1
list ht_capab DSSS_CCK-40

config wifi-iface
option device   radio0
option network  lan
option mode     sta
option ssid     CRap05
option wds 1
```

B.3.2 Network configuration

```
#/etc/config/network Rx

config interface 'loopback'
option ifname 'lo'
option proto 'static'
option ipaddr '127.0.0.1'
option netmask '255.0.0.0'

config interface 'lan'
option ifname 'eth0.1'
# option type 'bridge'
option proto 'static'
option ipaddr '192.168.0.75'
option netmask '255.255.255.0'

config interface 'wan'
option ifname 'eth1'
option proto 'dhcp'

config switch
option name 'rtl8366s'
option reset '1'
option enable_vlan '1'

config switch_vlan
option device 'rtl8366s'
option vlan '1'
option ports '0 1 2 3 5t'
```

Appendix C

Scripts

C.1 Data collection sample script

```
#!/bin/sh
x=1
location="$1"
while [ $x -le 5 ]
do
   tcpdump -tttt -c 1000 -i mon0 -w Meas-ISM-$location-$x.dump
                '(ether host 00:18:e7:da:a4:2a)&&link[0]==0x80'
   echo "ISM Location $location, File number $x, capture finished!"
   x=‘expr $x + 1‘
done
```

C.2 Data processing script

```
#!/bin/sh
FILES="Meas-*.dump"
for f in $FILES
do
name="${f%.*}-rssi"
tcpdump -nettvvv -s 0 -r $f > $f.txt
awk '{print $9}' $f.txt > $name.txt
rm $f.txt
done
```

Appendix D

Measurement location maps

The maps below were downloaded from Open Street Map. The markers were added by Radio Mobile - RF propagation simulation software. The first map contains all the measured locations which marked with red flag with location number below. Since too many measurement locations around the Otaniemi Open Innovation (OIH) building, we took OIH building as a center and zoomed part of the first map as the second map below.

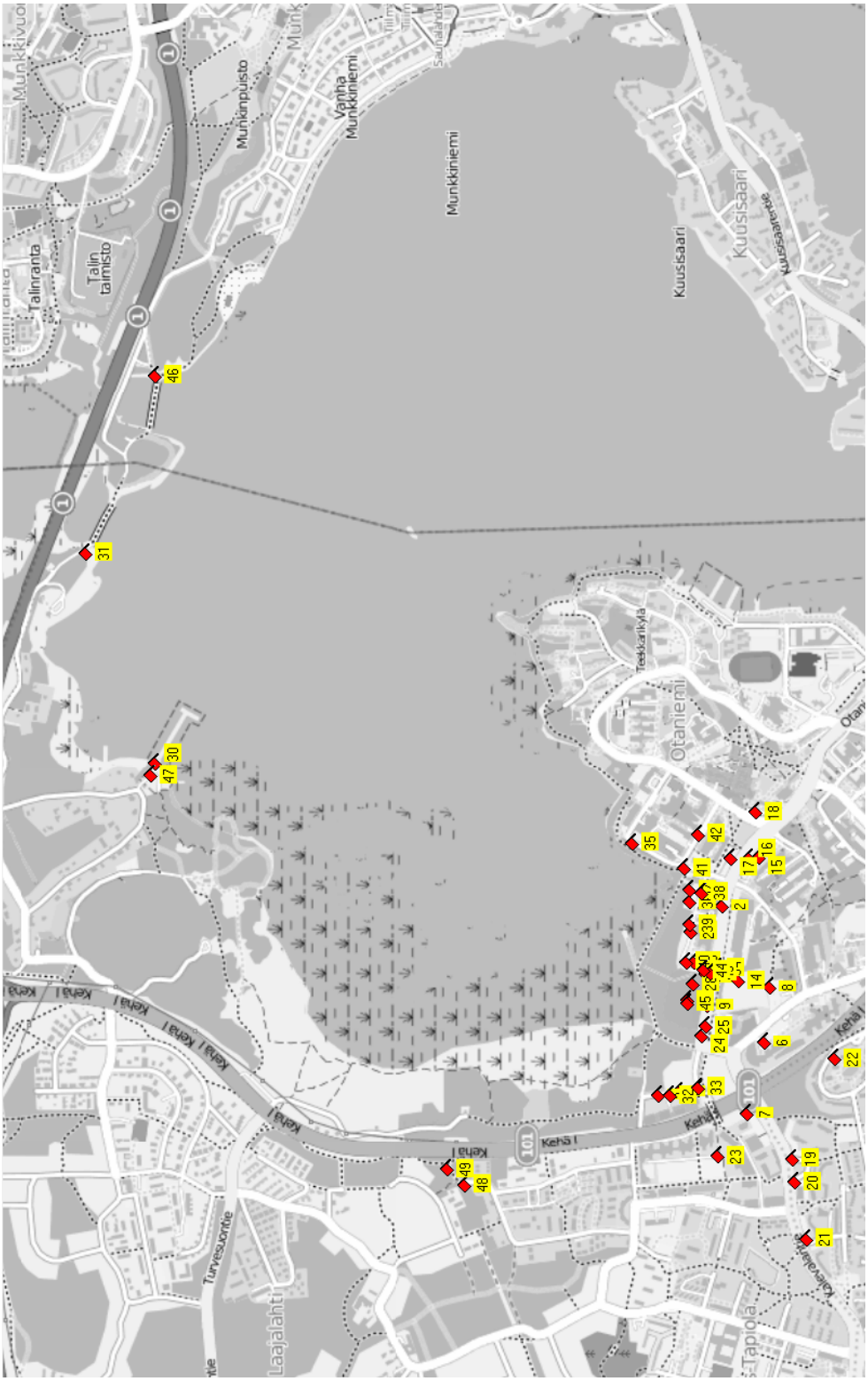

Figure D.1: Location data

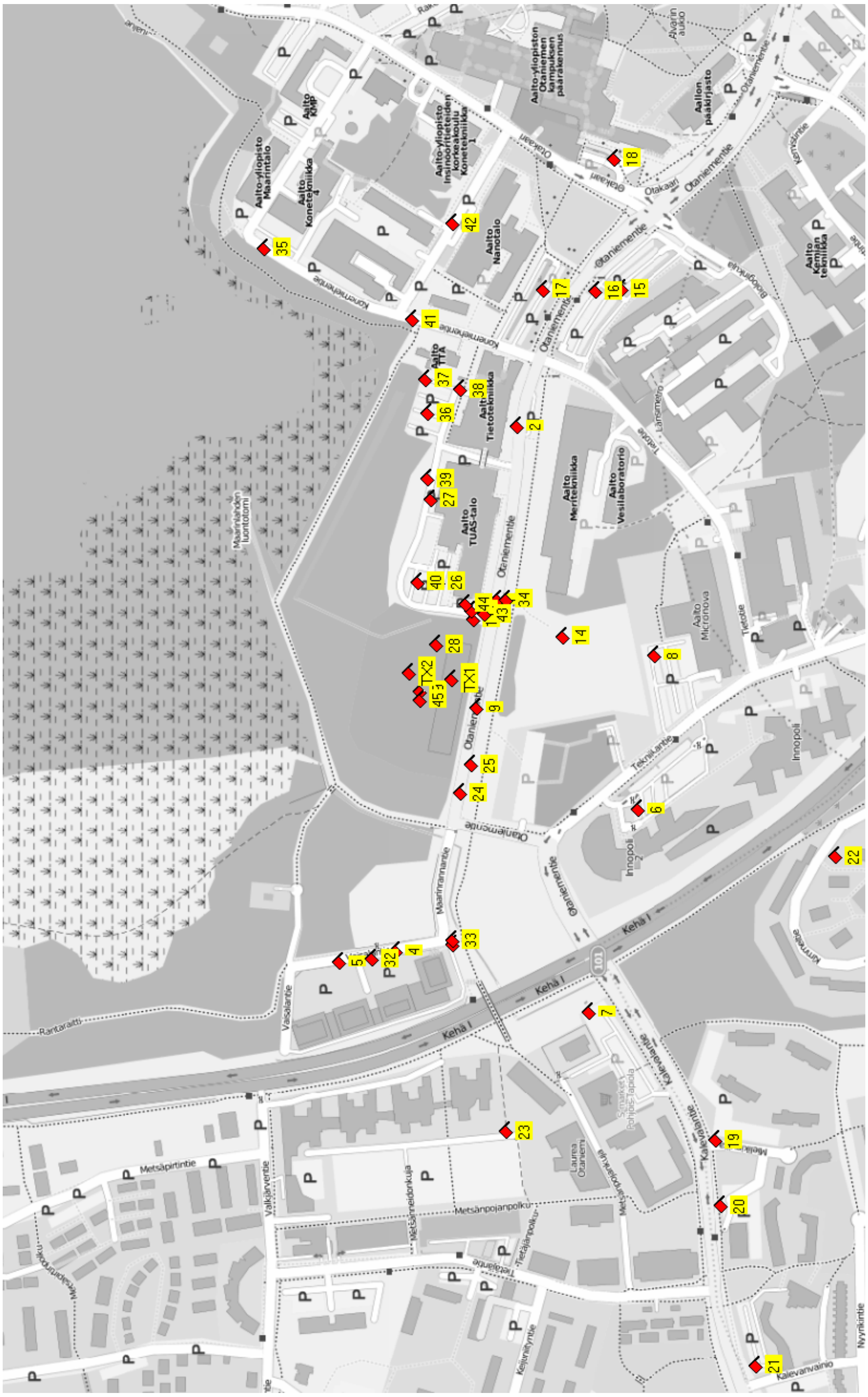

Figure D.2: Location data (zoom)